

Contents lists available at ScienceDirect

# International Journal of Naval Architecture and Ocean Engineering

journal homepage: www.journals.elsevier.com/international-journal-of-naval--architecture-and-ocean-engineering/





# A CII-oriented ship routing framework based on probabilistic decarbonization compliance

Qikun Wei a,b, Yan Liu a, You Dong b, Meixia Chen a

- <sup>a</sup> School of Naval Architecture and Ocean Engineering, Huazhong University of Science and Technology, Wuhan, China
- b Department of Civil and Environmental Engineering, The Hong Kong Polytechnic University, Hong Kong, China

#### ARTICLE INFO

Keywords:
Ship routing
Decarbonization
Regulatory compliance
Carbon intensity indicators

#### ABSTRACT

A low-carbon future is inevitable. As part of the global transition, the International Maritime Organization has implemented an ambitious decarbonization strategy since 2011. The Carbon Intensity Indicator (CII) serves as a crucial and up-to-date regulatory index for reducing greenhouse gas emissions in maritime transportation. Considering that CII is an annual indicator, there is room for adjustment on a single voyage based on different preferences. A novel cumulative compliance probability of CII is proposed to improve the performance of decarbonization for ship routing. An improved dynamic programming algorithm is applied to ship routing. Different sources of data and models, including weather data, are effectively integrated into the developed ship routing framework. The proposed framework provides intuitive insight into the condition of compliance of CII for ship stakeholders from an annual perspective. The framework is flexible and adjustable based on different preferences and is illustrated with a container ship case.

#### 1. Introduction

The world has seen a rapid transition to a lower carbon future. As the shipping industry carries more than 80% of international transportation, carbon reduction of shipping is an essential component of the global move. Studies on ship emissions have been conducted extensively (You and Lee, 2022). To accelerate the pace of reducing carbon emissions, a revised IMO GHG (Greenhouse Gas) Strategy, including enhanced targets to tackle harmful carbon emissions, has been adopted by the International Maritime Organization (IMO) (MEPC, 2023). Meanwhile, a new mandatory decarbonization regulation, namely the Carbon Intensity Indicator(CII), has come into effect since 2023, which has attracted great attention from the maritime industry.

All international new and existing vessels above 5000GT are under the supervision of CII. Revised and improved Ship Energy Efficiency Management Plan (SEEMP) are required for ships that fail to meet the criteria of CII, describing how carbon emissions will be reduced (MEPC, 2021). The regulation has aroused widespread investigation in the maritime industry, including new vessels (Han et al., 2024), retrofits (Bayramoğlu, 2024), and assessments of existing vessels (Bayraktar and Yuksel, 2023). In addition, other potential negative impacts of ships with poor CII performance have to be considered, such as damage to the reputation of stakeholders, reduced charter rates and resale values, business scope reduction, rising financing expenses due to CII being part of financial institutions' lending criteria, and increasing insurance

premiums. Therefore, the necessity and significance of CII management for shipping operations cannot be overemphasized.

Decision-making of ship routing is a complex system on account of numerous relevant elements and changing environments. A variety of elements have to be involved in shipping operation management, such as fuel consumption (Lashgari et al., 2021), port/canal congestion (Li et al., 2024; Wan et al., 2023), collision avoidance (Ha et al., 2024), fleet (Chua et al., 2023), Arctic navigation (Wang et al., 2025), global public crisis (Pan et al., 2022), safety (Guo et al., 2024), resilience (Gu et al., 2023), and algorithm (Jeong et al., 2025; Tang et al., 2024). Ship routing is naturally applicable for CII management as it directly affects fuel consumption and carbon emissions (Borén et al., 2022; Moradi et al., 2022). Therefore, considerable attention has been raised apace to reducing and managing CII by ship routing. Sun et al. (2022) introduced wind-assisted rotors into an A\* algorithm-based ship routing framework for optimal sailing routes. Tsai and Lin (2023) discussed the relationship between the output power and Attained CII of ships and further analyzed how the CII rating mechanism affects the development of the northeast passage. Mannarini et al. (2021) computed the least carbon emissions routes of ferries in the Adriatic Sea based on CII regulations. Yuan et al. (2023) developed a model to optimize annual fleet profits with various shipping characteristics incorporated while maintaining all vessels in legal CII rating status. Speed (Elkafas et al.,

E-mail addresses: weiqikun@hust.edu.cn (Q. Wei), yanliuch@hust.edu.cn (Y. Liu).

Corresponding author.

2023; Sun et al., 2023), safety (Jon and Yu, 2023), and other elements (Tran et al., 2023) are investigated to optimize CII as well. The above studies have studied in depth the approaches to cut carbon emissions and improve energy efficiency based on ship routing. These studies extend the methods of investigating past decarbonization indicators to the study of CII, which would still make significant progress in carbon reduction. However, the characteristics of CII differed from past indicators have not been concerned, i.e., the CII rating system. The characteristics of the CII rating system are studied in this work to improve the applicability of the proposed framework.

The implementation of the CII rating mechanism not only strengthens supervision but also gives stakeholders the opportunity to reduce costs. This is because a single rating in the rating mechanism corresponds to a range of carbon intensity values. It means that better and worse energy efficiency performances among the range of a single rating are the same as the annual CII assessment. In other words, this effort to reduce emissions was wasted by not achieving a higher rating from the economic perspective. Hence, opportunities could be seized to reduce this waste and reduce costs consequently.

To the best of the authors' knowledge, the studies of decarbonization optimization for ship routing could be divided into two categories: long-term perspective studies based on annual/life-cycle indicators (Irena et al., 2021; Hua et al., 2024) and short-term perspective studies based on real-time/short-term indicators (Wei et al., 2023; Li et al., 2020). Most long-term studies are conducted based on collected historical data. However, it is hysteretic for current management as real-time/predicted shipping data is not involved. Real-time/predicted data on environmental change is indispensable for ship routing. This problem has been investigated in short-term studies where the shipping parameters of a single voyage are optimized. Nevertheless, from an annual perspective of ship routing, it may over-cut carbon emissions under the specific supervision of that year and lead to profit reduction. Therefore, a novel cumulative compliance probability of CII(CCPC) is introduced herein to solve the mismatch between short-term ship routing and the annual indicator of regulatory supervision. By combining historical and real-time emissions data, CCPC provides a comprehensive decarbonization management perspective that includes both annual and short-term perspectives. Distinguished from technical indicators of decarbonization or energy efficiency measurement, the CCPC reveals operational risk concerning carbon reduction in the form of probability, which intuitively demonstrates the current pressure to reduce carbon emissions. The former is changing in real-time according to sea conditions however, the latter is being evaluated from a long-term perspective. The CCPC reflects current decarbonization compliance based on an annual assessment perspective by accumulating carbon emissions since the beginning of a supervisory year. Herein, CCPC is introduced to help seize opportunities to reduce costs based on the specific standard of CII.

The transportation cost and risk of violating decarbonization regulations are introduced in the present study for the analysis of ship routing. A multi-criteria optimization model is established to seek a balance between cost and risk. Decision-making preference is introduced to improve the multi-criteria model. The optimal strategy is derived based on the preferences of different stakeholders. The model enhances the decarbonization initiatives of the proposed ship routing framework.

This study aims to develop a ship routing framework adapted to CII for enhancing the decarbonization management of shipping operations based on the novel CCPC indicator. The proposed framework could reduce shipping costs with a CII rating maintained based on regulatory standards, which stakeholders preferred. The developed framework enhances the initiatives for annual decarbonization management of CII based on CCPC. It is conducive to improving ships' ability to cope with the supervision of CII. The paper is organized as follows: Section 2 presents the methodology utilized for the framework establishment. Two case studies of a container ship are illustrated in Section 3. The conclusions of this study are summarized in Section 4.

#### 2. Methods

#### 2.1. Multi-criteria framework

A multi-criteria ship routing framework is established in this part, as presented in Fig. 1. The framework finally outputs an optimized route by applying the input real-time environmental data of sea conditions. The input consists of four components: ocean data, weather data, port data, and position. Ocean data is utilized to form a gridded sea map containing information on ocean, land, and islands. Weather data mainly includes wave and wind data, which are used to calculate the carbon emissions of vessels. Port data includes departure port and destination port, which are utilized to define the initialization and termination of the shipping task. Position means the position of the ship on the gridded sea map. The position is used to mark the state of the framework, i.e., the framework would be updated as the position is updated. This framework mainly consists of four components: ship routing model, CCPC model, multi-criteria model, and carbon emission model. The CCPC model updates the state of carbon emissions level according to the historical data from the ship routing model. Then, according to the standards of CII regulations, the CCPC model assesses the compliance of every position in the navigation area. The carbon emission model is used to provide predicted carbon emissions for the CCPC model. In the multi-criteria model, shipping cost is integrated with CCPC into the multi-criteria function to seize opportunities to cut vessels' operational costs within the CII rating maintained. Decision preferences are concerned in this model to improve the applicability of the proposed framework. A final sea map containing multi-criteria information is applied for ship routing. The ship routing model is used for searching the shipping path with the optimal sum of multi-criteria values based on several inputs. The cumulative calculated results are acquired for the next cycle. Meanwhile, current decision-making support is output, including optimized route and tracking of CII rating. The detailed procedures of this ship routing framework are demonstrated from Sections 2.2 to 2.6.

#### 2.2. Carbon intensity indicator

The Carbon Intensity Indicator (CII) is the main mandatory decarbonization regulation for international shipping currently. CII applies to almost all internationally transporting ships of 5000 GT and above and has been coming into force since 2023. Attained CII and Required CII are two crucial components of CII regulations. They represent the carbon intensity of vessels and the standard baseline of regulations, respectively. It should be noted that the standard of CII is tightened over time. This may lead to some ships that comply with regulations currently failing to be compliant in the future, as illustrated in Fig. 2.

#### 2.2.1. CII calculation

Attained CII indicates the annual energy efficiency of ships in the form of a ratio as shown in Eq. (1) (MEPC, 2022b).

$$AttainedCII = M/W (1)$$

where M is the total mass of  $CO_2$  emissions(in grams), and W is the total transport work(in tons · nautical miles). The M is calculated by fuel consumption multiplied by the  $CO_2$  emissions factor. The transport work is determined by distance sailed and deadweight or GT.

The *Required CII* is a standard value that decreases over the years. It can be derived from the reference line of CII and reduction factors as presented in Eqs. (2) and (3).

$$RequiredCII = (1 - Z/100) \times CII_{ref}$$
 (2)

where Z is the reduction factor and equals 5, 7, 9, and 11, respectively, from 2023 to 2026 (MEPC, 2022a). The  $CII_{ref}$  is the reference line in

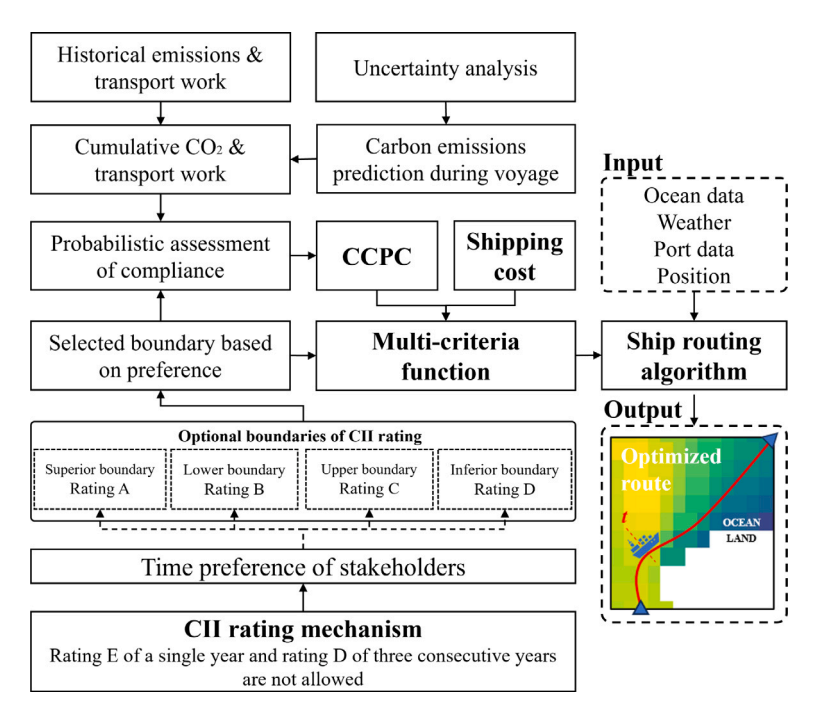


Fig. 1. Workflow diagram of the proposed framework.

the year 2019 according to MEPC (2022c), and it is derived as follows equation.

$$CII_{ref} = aCapacity^{-c} (3)$$

where Capacity usually equals to the dead weight tons(DWT) of ships. The a and c are fitted parameters estimated based on sample data of 2019, which could be acquired from IMO files (MEPC, 2022c).

# 2.2.2. CII rating mechanism

A rating system is introduced into the CII regulations for the assessment of ships' energy efficiency, as shown in Fig. 2. Each vessel to which CII regulations apply is annually given a ranking label from rating A to rating E based on the *Attained CII* (MEPC, 2022d). The rating assessment is conducted on ships for each calendar year. A ranking label of A, B, or C means the vessel satisfies current regulations and passes the assessment. If a ship gets an E for one year or three consecutive D ratings, it has to propose and implement a corrective plan for upgrading the CII rating (MEPC, 2021). As presented in Fig. 2, the A to E rates are divided by four boundaries, namely superior boundary, lower boundary, upper boundary, and inferior boundary, which are calculated based on *Required CII* and deviation vectors (MEPC, 2022d).

# 2.3. Cumulative compliance probability of CII

CII has attracted widespread attention in the marine industry and academia with the worldwide burgeoning sustainable development. However, the introduction of a rating system distinguishes CII from previous decarbonization indicators, not merely comparing the actual value of energy efficiency and regulatory standards. Hence, a novel indicator/method applying to CII is presently essential for supporting the decision-making of shipping operations. The proposed CCPC is illustrated in this section, and this part is organized as follows. The assessment of decarbonization compliance, i.e., the calculation method of CCPC, is described in 2.3.1. Relevant physical methods and equations are clarified in 2.3.2.

#### 2.3.1. Calculation of compliance

CII is an annual indicator for long-term evaluation and supervision, which cannot be implemented into real-time ship routing directly. Hence, the calculating procedure of CII is introduced to acquire the carbon intensity of a specific period, which can be seen as a variant of  $Attained\ CII$ . The carbon intensity is written as Real-time CII. The calculating procedure for Real-time CII is the same as  $Attained\ CII$ , just changing the time of M and W from a calendar year to a short period.

$$Real - timeCII = M_t/W_t \tag{4}$$

According to the physical model, the obtained *Real-time CII* is in a prediction interval that includes a predictive mean value. Herein, *Real-time CII* is assumed to obey a fitted probability distribution in the prediction interval, and the mean of the probability distribution equals the predictive mean value. As illustrated in Fig. 3, after the distribution for *Real-time CII* of a particular time is derived, the probability of a specific carbon intensity can be derived. When the specific CII value equals the standard lines of CII regulations, the obtained probability indicates the compliance of CII in the given time. The equation is presented as follows.

$$C_{Real-time} = P(Real - timeCII \le S_{CII}) = \int_{-\infty}^{S_{CII}} F$$
 (5)

where  $C_{\textit{Real-time}}$  is the compliance of CII in a short period,  $S_{CII}$  is the value of regulatory standard, and F is the probability density function. It should be noted that the  $S_{CII}$  is not Required CII but the four CII rating boundaries. The selection of  $S_{CII}$  from four boundaries is up to the decision of the stakeholders of vessels. The upper and inferior boundaries are mainly employed in this study to meet the minimum requirements of regulations.

On the basis of  $C_{Real-time}$ , historical carbon emissions and transport work are introduced to indicate the cumulative compliance level from past to present, namely CCPC. The definition of the 'past' is flexible; it can be either the early part of a single navigation or the first few months of the year. The equation of CCPC is presented as follows.

$$CCPC = P(\frac{M_t + M_h}{W_t + W_h} \le S_{CII})$$
 (6)

where  $M_t$  and  $M_h$  are carbon emissions at present and historical emissions, respectively, and  $W_t$  and  $W_h$  are current transport work and

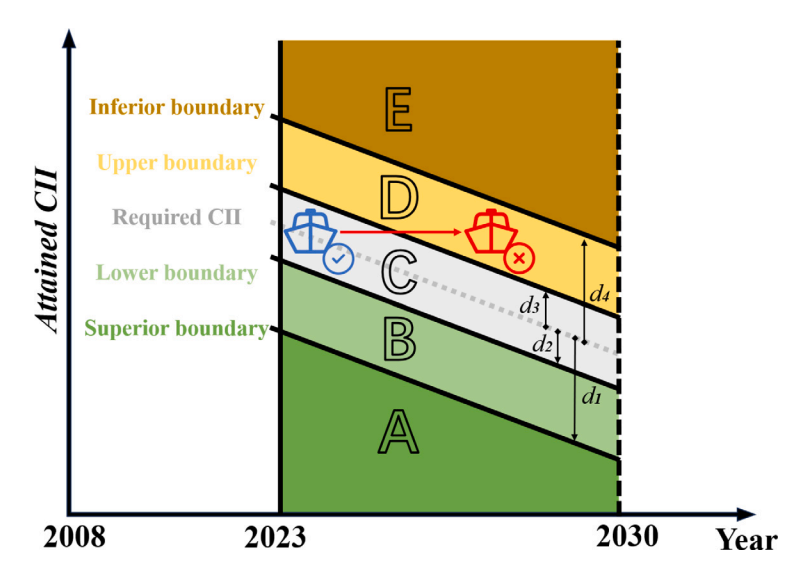


Fig. 2. The CII rating system over the years.

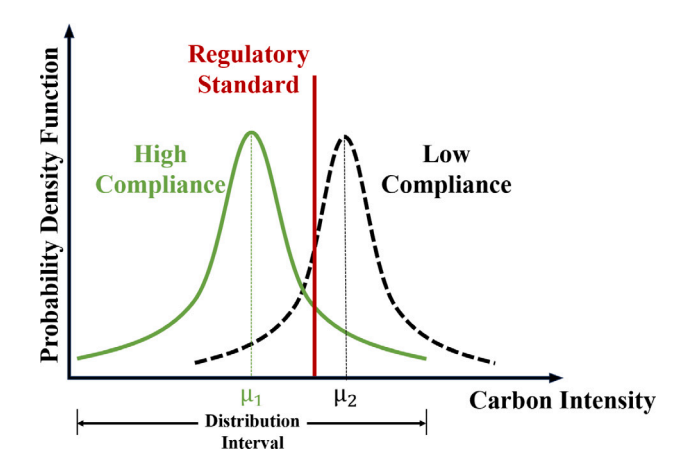


Fig. 3. The schematic diagram of compliance calculation.

transport work in the past. CCPC indicates the compliance level in the proposed framework. Hence, 1-CCPC reveals the regulatory risk in the same perspective. The probability of CCPC is derived from uncertainty and error in the calculation, which is mainly from the prediction of carbon emissions.

#### 2.3.2. Carbon emission model

This section presents the prediction procedure of  $\mathrm{CO}_2$  emissions based on real-time sea conditions during a voyage. The  $\mathrm{CO}_2$  emissions could be derived from the fuel consumption of ships, which is determined by engine power and running time. The engine power, including main engines and auxiliary engines, can be obtained by navigation records such as noon data. However, the data is difficult to acquire from shipping enterprises, and this approach is hysteretic for real-time ship routing support. Herein, a resistance model based on real-time sea conditions is established to estimate engine power.

#### (1) CO<sub>2</sub> emissions and fuel consumption

According to the calculating guidelines of CII,  $\mathrm{CO}_2$  emissions are determined by fuel consumption and carbon conversion factor as follows.

$$M = \sum_{j \in J} FC_j \times C_{Fj} \tag{7}$$

where j is the type of fuel oil, J represents the set of all types of fuel oil used in a voyage, FC means the total mass of fuel consumption(in

grams), and  $C_F$  is a factor indicating the  $CO_2$  emissions(in grams) per unit of fuel oil and the  $C_F$  is determined according to the type of fuel.

There are many sources of fuel oil consumption onboard in practice; herein, main engines and auxiliary engines are concerned as presented in Eq. (8).

$$FC = \sum_{i} \sum_{i} SFOC_{i} \times P_{E \ i} \times t \tag{8}$$

where i is the type of engines, n is the number of engines, SFOC is the specific fuel oil consumption index, which represents the mass of fuel oil consumed per unit energy,  $P_E$  is the engine power, and t is the running time.

#### (2) Power model

As stated above, the main engines and auxiliary engines are introduced into the power model. The main engine power in this model is the output shaft power. It can be derived by the effective power of the propeller and delivery efficiency of shafting, as presented in Eq. (9).

$$P_{E(M)} = \frac{P_e}{\eta_H \eta_0 \eta_R \eta_S} \tag{9}$$

where  $P_{E(M)}$  is the power of main engines,  $P_e$  represents the effective power of vessels,  $\eta_H$ ,  $\eta_0$ ,  $\eta_R$ ,  $\eta_S$  represent the effects of the hull, propeller and shaft system on power transmission efficiency respectively.

The effective power represents the situation in which ships sail against resistance in real sea conditions. It can be derived by sailing speed and total resistance encountered as follows.

$$P_{\rho} = R_{t} \times U \tag{10}$$

where  $R_t$  represents the total resistance of vessels, and U is speed(in knot). As the involuntary speed caused by environmental conditions has been involved in the wave and wind added resistance calculation procedures, the speed is assumed to be constant. The voluntary speed loss caused by human factors and emergency circumstances during navigation is not considered herein.

Hull efficiency  $\eta_H$  could be calculated as Eq. (11), where  $f_t$  is the thrust deduction factor and w is the wake fraction.

$$\eta_H = \frac{1 - f_t}{1 - w} \tag{11}$$

The open water efficiency  $\eta_0$  could be obtained directly through a propeller open water test and is expressed by the thrust coefficient, torque coefficient, and advance ratio. The  $\eta_0$  in 3 is obtained from literature (Seo et al., 2010) since no test or simulation is conducted. Relative rotational efficiency  $\eta_R$  is suggested to be an average value of 1.0, which often ranges from 0.98 to 1.05 (Sheng and Liu, 2004).

Shafting efficiency  $\eta_S$  is suggested to be 0.98 (Sheng and Liu, 2004). Herein,  $\eta_R$  and  $\eta_S$  are assumed to be 1.0 and 0.98, respectively.

The auxiliary engines take auxiliary functions other than propulsion, such as generating electricity. The total power of auxiliary engines  $P_{E(A)}$  is difficult to derive due to the wide variety of engines for various functions and requirements of different ship types. Conventionally, empirical formulas based on ship size or main engine power are used for estimating auxiliary power. However, the results of empirical formulas estimation based on ship size or other main parameters are not necessarily valid (Goldsworthy and Goldsworthy, 2019). Considering that the auxiliary engine power is uncertain without actual ship data, herein, a probabilistic distribution fitted by real ship data is established to acquire the  $P_{E(A)}$ ,  $P_{E(A)} \sim f(X)$ . f(X) is the fitted distribution based on actual ship data and X is random variable. Herein, the TEU is introduced as a random variable. The detailed information and calculation procedure are presented in Section 2.3.3.

#### (3) Resistance model

The total resistance of vessels could be divided into calm water resistance  $R_c$  and added resistance  $R_a$ . The former represents the resistance encountered in calm water. It is determined by hull shape lines and speed in real shipping operations. Conventionally, the calm water resistance can be derived by scaled model tests or ship trials. An empirical formula is introduced herein to enhance the applicability of the resistance model as follows.

$$R_c = \frac{1}{2}\rho C_T U^2 S_0 \tag{12}$$

where  $\rho$  is the density of sea water,  $C_T$  is the total drag coefficient, and  $S_0$  is the wetted surface area.  $C_T$  could be obtained by model tests or CFD simulations (Islam et al., 2017).

Added resistance is generated by additional environmental factors in real sea conditions, such as waves, wind, currents, etc. As the main source of added resistance, the resistance caused by waves is considered. The wave added resistance is difficult to derive because the sea conditions are changing rapidly and the coupling of wave and hull is complex. The analytical solution of wave added resistance is not applicable for the tremendous amount of calculation. Therefore, a semi-empirical formula proposed by Liu and Papanikolaou (2020) is introduced herein, which is beneficial to data-driven massive calculation. It has to be noted that this method has been adopted in ISO 15016:2025. The wave added resistance could be written as follows.

$$R_{awave} = \frac{C_{AW} \rho g \zeta_A^2 B^2}{L} \tag{13}$$

where  $C_{\rm AW}$  represents added resistance coefficient(dimensionless),  $\zeta_{\rm A}$  is wave amplitude, B and L are breadth and length respectively. The detailed methods and calculating procedure can be found in Mittendorf et al. (2022).

This approach to wave added resistance based on a semi-empirical formula is appropriate for arbitrary wave directions (Liu and Papanikolaou, 2020). Hence, Eq. (13) is convenient to use to deal with complex wave data in real sea conditions. According to the calculating procedure in Mittendorf et al. (2022)'s work, the wave added resistance is obtained in the form of a tuple, a mean value, and a 90% prediction interval. Herein, the wave added resistance is assumed as normally distributed with a mean equal to the predicted mean resistance.

The wind added resistance is affected by the shape of the hull and structures above the deck. The increased resistance  $R_{awind}$  could be derived by the following equation (ISO, 2015).

$$R_{awind} = 0.5\rho_{air} \cdot C_{AA} \left( \psi_{WRref} \right) \cdot A_{XV} \cdot V_{WRref}^2 - 0.5\rho_{A} \cdot C_{AA}(0) \cdot A_{XV} \cdot U^2$$
 (14)

where  $\rho_{air}$  is the air mass density,  $\psi_{WRref}$  denotes the relative wind direction,  $C_{AA}(\psi_{WRref})$  represents the wind resistance coefficient for a corresponding wind direction  $\psi_{WRref}$ ,  $C_{AA}(0)$  means the wind resistance coefficient in head wind,  $A_{XV}$  is the transverse projected area above the waterline including superstructures, and  $V_{WRref}$  is the

relative wind velocity.  $C_{\rm AA}(\psi_{\rm WRref})$  and  $V_{\rm WRref}$  are two variables in Eq. (14).  $C_{\rm AA}(\psi_{\rm WRref})$  is a coefficient based on wind direction. Therefore, the wind added resistance could be acquired based on wind direction and wind velocity according to Eq. (14). The wind direction and wind velocity data are obtained from Deutscher Wetterdienst (DWD) (Wetterdienst, 2023).

#### 2.3.3. Uncertainty model

Uncertainties are unavoidable in the calculation procedure of carbon emission prediction. The quantification of uncertainties is the foundation of the calculation of compliance. From the perspective of the production of carbon emissions, the uncertainty of fuel-burning equipment needs to be quantified. Herein, the main engine and auxiliary engine are seen as the uncertainty sources as they produce the vast majority of carbon emissions. Boilers, marine generators, and other non-main equipment are not considered for the simplification of calculation.

#### (1) Uncertainty of main engine power

In the calculation procedure of carbon emission estimation for the main engine, uncertainty comes from the resistance model. In the resistance model, uncertainty exists as empirical formulas are used. For calm water resistance, the key index  $C_T$  is acquired from model tests or CFD simulations, which is stable for mature ship types. For added resistance, wave added resistance accounts for most of the added resistance. Hence, the uncertainty of wave added resistance is considered herein.

In Eq. (13),  $C_{\rm AW}$  is the dimensionless parameter that characterizes the wave added resistance. The analysis for the uncertainty of  $C_{\rm AW}$  is necessary as the selection of  $C_{\rm AW}$  is based on empirical formulas and data fitting. Other parameters in Eq. (13) are constants or input data. Possible errors in these parameters are beyond the scope of this paper. Therefore,  $C_{\rm AW}$  is seen as the uncertainty source of wave added resistance calculation. The sample data of  $C_{\rm AW}$  is summarized from literature (Mittendorf et al., 2022) for probability distribution fitting, as shown in Fig. 4. It has to be noted that Mittendorf et al. (2022) has analyzed and expressed the uncertainty of the semi-empirical added resistance formulas. Their study gave 90% prediction interval of the added resistance results. However, the probabilistic distribution in the prediction interval is not given. Based on Mittendorf et al. (2022)'s study, this section establishes a probabilistic distribution to further express the uncertainty in the prediction interval.

Conventionally, the  $C_{\mathrm{AW}}$  is classified according to relative heading. Seven relative heading scenarios, i.e., 0, 30, 60, 90, 120, 150, and 180, are set in this section. For each relative heading, appropriate intervals are divided according to the number of samples. Herein, the interval length is 0.2 and 0.5 for 180 deg and other headings, respectively. Eleven distributions are introduced for probability distribution fitting based on the sample data in each interval, such as the red frame in Fig. 4. The sum of squares due to error(SSE), Akaike information criterion(AIC), and Bayesian information criterion (BIC) are introduced to evaluate the fitted distribution. The smaller the SSE, AIC, and BIC are, the better the probability distribution is. Hence, the sum of SSE, AIC, and BIC of each fitted distribution is used for verification. On account of the difference in the value range of the three indexes, normalization processing is necessary before verification. The detailed uncertainty analysis is divided into two steps. First, the normalized SSE, AIC, and BIC are calculated for each interval for each heading, as presented in Table 1. Second, the normalized results of all intervals in one heading are added together as presented in Table A.1 in the Appendix. According to the results in Table A.1, the beta distribution could be determined as the most suitable probability distribution for heading = 180 deg. The normalized results of other headings can be found in the Appendix. The results of the distribution fitting and analysis for each heading are shown in Table A.2 in the Appendix. It could be found that the sum value of the beta distribution is the lowest.

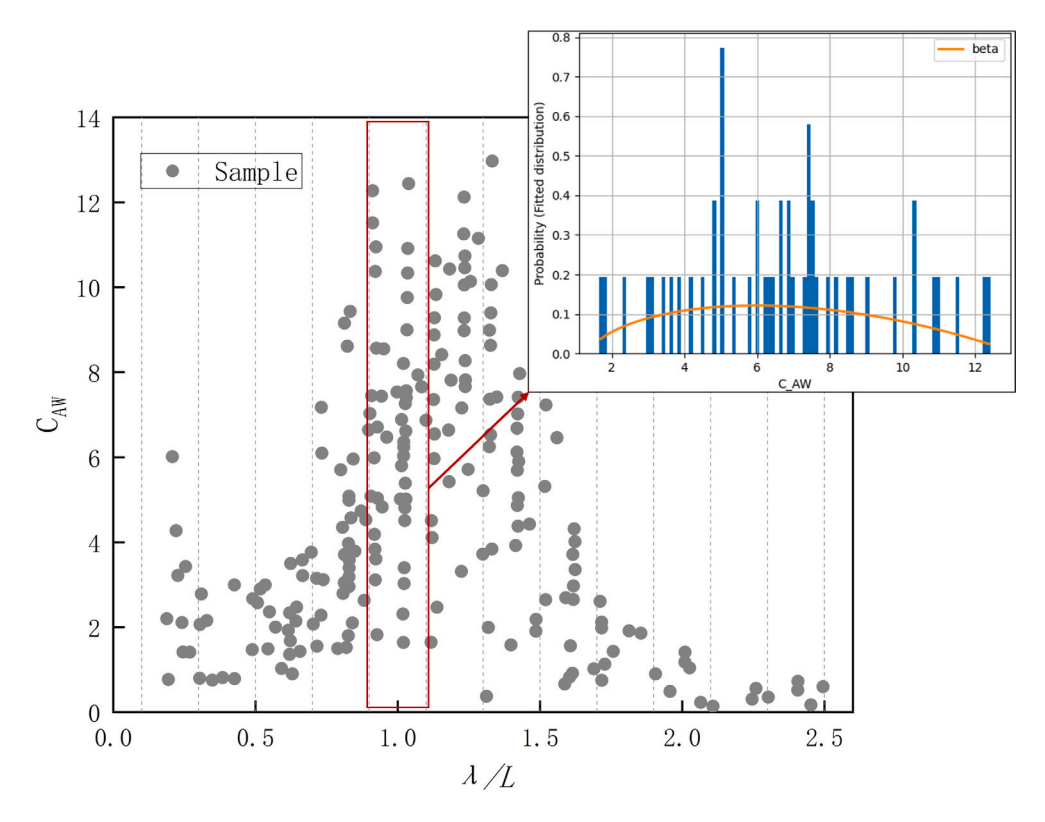


Fig. 4. Samples scatter plot of added resistance coefficient when relative heading equals to 180 degrees and the data comes from Mittendorf et al. (2022)'s research. The probability distribution of  $C_{AW}$  is segmentally fitted based on the ratio of wavelength to ship length.

Table 1

Normalized evaluation parameters of eleven distribution when the relative heading is 180 and the interval is from 0.1 to 0.3.

	Alpha	Beta	Cauchy	Gamma	d-gamma	Normal	log-normal	$\mathcal{X}^2$	Weibull	e-weibull	d-weibull
SSE	0.13	0.00	0.27	0.02	0.01	0.24	0.11	0.04	1.00	0.05	0.07
AIC	0.21	0.00	0.51	0.34	0.27	0.14	0.21	0.43	1.00	0.35	0.17
BIC	0.21	0.00	0.51	0.34	0.27	0.13	0.21	0.43	1.00	0.35	0.16
SUM	0.55	0.00	1.29	0.70	0.55	0.51	0.53	0.90	3.00	0.75	0.40

Therefore, the beta distribution is used to fit the distribution of  $C_{\rm AW}$  as follows.

$$C_{\rm AW} \sim Beta(\alpha, \beta)$$
 (15)

where  $\alpha$  and  $\beta$  are the parameters of beta distribution and are acquired by data fitting. The detailed parameters of each beta distribution for seven headings are listed in Table A.4 in the Appendix.

# (2) Uncertainty of auxiliary engine power

The installed auxiliary power of each ship is different as the auxiliary machines need to bear different loads. As mentioned above in Section 2.3.2, statistical data is introduced to fit a probabilistic distribution for auxiliary power estimation, and the data comes from Goldsworthy and Goldsworthy (2019)'s work. Goldsworthy and Goldsworthy (2019) sorted out the literature data and investigated some actual ship data, and some of the data for container ships are shown in Fig. 5.

The data is introduced to fit the probability distribution of  $P_{E(A)}$ . According to the comparison of fitted distribution error, the beta distribution is used as the probability distribution for  $P_{E(A)}$  estimation. The four parameters of the fitted beta distribution,  $\alpha$ ,  $\beta$ , location, and scale, are 1.79, 0.70, 567.03, and 996.97, respectively, where location and scale are scaling factors since the standard beta distribution is defined in the range 0 to 1. It has to be noticed that for a specific vessel, the uncertainty analysis of the auxiliary engine power could be replaced by an analysis based on its auxiliary engine historical data. The replacement could enhance the applicability of the proposed framework in specific scenarios and would not weaken the effectiveness of the framework since it is built based on various functional modules.

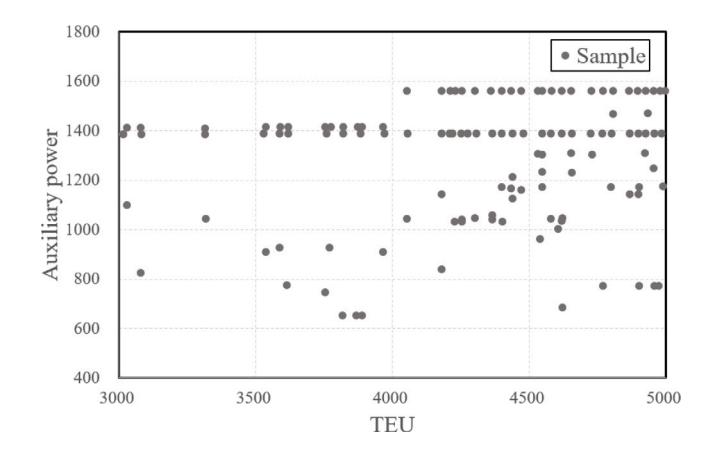


Fig. 5. The  $P_{E(A)}$  data of container ship from 3000 TEU to 5000 TEU (Goldsworthy and Goldsworthy, 2019).

#### 2.4. Shipping cost

The shipping cost can be divided into three components (Sheng et al., 2019): fuel cost  $Cost_t$ , in-transit cargo inventory cost  $Cost_i$ , and non-fuel vessel operating cost  $Cost_o$ , as follows.

$$Cost_t = Cost_f + Cost_i + Cost_o (16)$$

$$I_{c(i,j)} = \frac{Cost_{t(i,j)} - \min(Cost_{t(\delta_0,\gamma_0)}, \dots, Cost_{t(i,j)}, \dots, Cost_{t(\delta,\gamma)})}{\max(Cost_{t(\delta_0,\gamma_0)}, \dots, Cost_{t(i,j)}, \dots, Cost_{t(\delta_0,\gamma_0)}, \dots, Cost_{t(\delta,\gamma)})}$$

$$(20)$$

Box I.

Fuel consumption is usually the major part of shipping costs. It can be calculated by the power of main and auxiliary engines as illustrated in Eq. (8). The in-transit cargo inventory cost is determined by cargo quantity and transport time. The non-fuel operating cost, i.e., fixed expenditure, is up to the inherent attributes of vessels. The calculating procedure of cost above for container ship is shown in Eqs. (17)–(19).

$$Cost_f = Pr_f FC \tag{17}$$

$$Cost_i = f_c t_t \cdot \text{TEU} \tag{18}$$

$$Cost_o = \frac{2.9186 \cdot \text{TEU} + 8122.2}{24} t_t \tag{19}$$

where  $Pr_f$  is the price of fuel oil(in USD),  $f_c$  is the cost factor of a single container,  $t_t$  represents the transport time, TEU means the total container quantity onboard, and the Eq. (19) is obtained by fitting the data of real ships in Sheng et al. (2019)'s study. Herein, the shipping cost is normalized for the multi-criteria function in Section 2.5 as Eq. (20) given in Box I, where  $I_c$  is the normalized index of shipping cost; (i,j) is the position of ship during navigation;  $(\delta_0,\gamma_0)$  is the coordinate of the departure point; and  $\delta$  and  $\gamma$  mean longitude and latitude of the entire voyage respectively.

#### 2.5. Multi-criteria function and decision preference

A multi-criteria function is introduced for the optimal decarbonization route with the shipping cost concerns within the restriction of CII regulations. The double metrics function, regulatory compliance, and shipping cost are expressed as follows.

$$F = 1 - CCPC + I_c$$
s.t.  $S_{CII} \in \{\text{superior boundary, lower boundary, upper boundary, inferior boundary}\}$  (21)

where  $I_c$  is the normalized index of shipping cost; 1-CCPC is directly employed in this non-dimensional equation due to CCPC is derived by probability density function, and  $S_{CII}$  is a parameter of CCPC defined in Section 2.3.1 which is determined by stakeholders' time preference.

Decision preference refers to the preference of decision-makers/ stakeholders based on risk. It depends on the decision makers' attitude towards acquired knowledge of CII compliance. Ship stakeholders have an incentive to be aggressive in sailing operations for more revenue when they believe decarbonization is less stressful. On the contrary, stakeholders will operate more conservatively if they are under pressure to cut carbon emissions. The preference is determined or affected by some other priorities outside of this study. Time preference (Cheng et al., 2020) is introduced as the decision preference of stakeholders in this study.

Time preference reflects stakeholders' attitudes towards to present and future. It can be described by formulas of delay in economics. However, as the CII rating system is discontinuous with decreasing rank boundaries, time preference is simplified as an adjustable ranking target. In this study, delay-taking represents ships that would meet the regulatory requirements of CII with minimum standards, postponing enforcement of stricter standards. Delay-averse means more stringent standards are adopted at present.

According to the regulations of CII, if a ship gets a D rating for three consecutive years or an E rating for a single year, it has to draw up an improved plan for upgrading the CII rating (MEPC, 2021), which causes additional costs and risks. Therefore, a D, D, and C rating sequence

in three consecutive years is an optional action for increasing current profits. From the perspective of time preference, the D-D-C sequence prefers the present to the future. In contrast, always maintaining a C, B, or even A rating is regarded as a forward-looking vision of carbon reduction. Herein, the upper boundary and inferior boundary are regarded as delay-averse and delay-taking, respectively.

# 2.6. Ship routing model

Ship routing is a classic but essential issue in shipping operations. Various methods and algorithms of ship routing have been developed for a long time, such as A star and Dijkstra algorithms (Kurosawa et al., 2020; Wang et al., 2019), which are common in practical applications. Dynamic programming is introduced to establish a route-searching algorithm.

Conventionally, ship routing is divided into ship scheduling and weather routing, and the latter is concerned herein. Weather data, such as wave data, is the foundation of ship weather routing. Wave spectra based on statistical data have been employed for weather routing in the past. With the rapid development of meteorological science and technology, the rapid acquisition of marine weather data has become a reality. Hence, weather ship routing has become an effective approach for reducing operating risks and emissions in complex sea conditions. This section describes the data-driven algorithm implemented for route searching.

#### 2.6.1. Data model

Weather data contains various elements in the actual oceans. Herein, wave and wind are applied to the ship weather routing, and other weather elements are not concerned in this study. Global wave and wind data are available from meteorological organizations nowadays. Meteorological institutions collect data from satellites, monitoring stations, buoys, and other measuring equipment. The data collected is used in the calculation of the global meteorological model for giving the global wave and wind data. Data herein is acquired from an open database of Deutscher Wetterdienst (DWD) (Wetterdienst). Model errors and other errors during the acquisition procedure of wave and wind data are not considered in this study as these issues belong to meteorological science.

Significant wave height(in meters), wave period(in seconds), wave and wind direction(in degrees), and wind velocity(in meters per second) are acquired from Wetterdienst. The data has been pre-processed and is regarded as accurate information. In data of wave and wind direction, 0 and 180 mean the wave and wind propagates due north and south, respectively. The data of significant wave height is the result of combined wind waves and swell as illustrated in Fig. 6. The wind velocity data from Wetterdienst is the wind speed at a height of 10 m.

#### 2.6.2. Route searching algorithm

The method of dynamic programming is employed in many fields to address intricate problems by breaking down the original problem into a series of sub-problems. Dynamic programming proves suitable for problems characterized by overlapping sub-problems and optimal substructure properties, offering the advantage of less time consumption. The optimal route problem from the starting point to the endpoint can be divided into several sub-problems: optimal route from starting point to intermediate points. The algorithm is expressed as follows.

$$\mathbb{F}_{i,j} = \min \sum_{i \in \mathcal{S}, j \in \gamma} \left( F_{i,j} + \min \left( \mathbb{F}_{i-1,j}, \mathbb{F}_{i-1,j-1}, \mathbb{F}_{i,j-1} \right) \right) \tag{22}$$

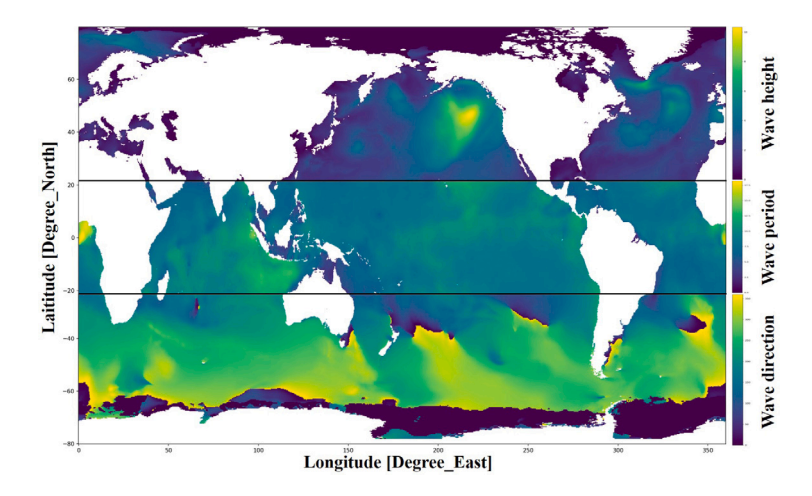


Fig. 6. Global wave data (Wetterdienst).

Table 2
Main parameters of the employed container ship.

Parameter	Lpp [m]	Lwl [m]	B [m]	D [m]	T [m]	Dis [m <sup>3</sup> ]	S [m] <sup>2</sup>	$C_B$	$C_M$	LCB [%]	U [Kn]
Value	230	232.5	32.2	19	10.8	52 030	9530	0.651	0.985	-1.48	13



(a) The trans-Indian Ocean route from Gqeberha to Banda Aceh.

(b) Liner shipping service between Shanghai and Busan

Fig. 7. Schematic diagram of two routes of case study (Esri).

Table 3
Main parameters of main engine and auxiliary engine (Kristensen, 2017).

Parameter	Fuel type	SFOC [kg/kW/hour]	$C_F$
Main engine	HFO	0.179	3.144
Auxiliary engine	MDO/GO	0.190	3.206

where  $\mathbb{F}_{i,j}$  represents the value of optimal route from starting point to position (i,j); the same goes for  $\mathbb{F}_{i-1,j}$ ,  $\mathbb{F}_{i-1,j-1}$ , and  $\mathbb{F}_{i,j-1}$ ;  $F_{i,j}$  is the result of multi-criteria function at position (i,j);  $\delta$  and  $\gamma$  mean longitude and latitude respectively.

The resolutions for longitude and latitude are both 0.25 degrees of data from Wetterdienst. Therefore, the grid of the sea map herein is constituted by massive  $0.25^{\circ} \times 0.25^{\circ}$  cells. The grid of the sea map is updated according to the time interval of Wetterdienst's data.

#### 3. Case study

Two routes are illustrated in this section to evaluate the effectiveness and applicability of the proposed framework, including a tramp route across the India Ocean and a liner traveling service between Shanghai and Busan. The wave and wind conditions of two routes are

different which are utilized to assess the applicability of the proposed framework.

# 3.1. Settings

As one of the three main ship types, container ships are more sensitive to decarbonization regulations on account of their higher speed than bulk carriers and tankers, and a container ship is employed herein for validation. The data of the ship is provided by the Korean Register of Shipping(KCS) (SIMMAN) is employed in this section. The main parameters of the container ship are organized in Table 2. The meanings of parameters in Table 2 that do not appear above are presented as follows: *Lpp* is the ship length between perpendiculars; Lwl is the ship waterline length; D is depth; T is draught; Dis is the displacement of ship; S is the wet surface of hull;  $C_B$  and  $C_M$  are ship block and midship section coefficients respectively; and LCB means the longitudinal buoyancy center. Speed U is determined to be 13 knots as Clarksons Research reported (Clarksons) that the average speed of global container ships was 13.72 knots in February 2023, and it would continue to decline. Detailed parameters and data about the rudder, propeller, appendages, and other essential components can be found in SIMMAN.

It has to be noted that the information of architecture on deck is not involved in SIMMAN. A similar ship, i.e., 3600 TEU container ship (Zhu

and Wu, 2021), is introduced to estimate the height of superstructures. Herein, the height is set at 5 m. The  $A_{\rm XV}$  in Eq. (14) could be estimated, i.e.  $A_{\rm XV} = (D-T+28) \times B$ . In addition, DWT, a key parameter of the CII calculation procedure, is not given by SIMMAN as well. DWT means the difference in tonnes between the displacement of a ship in water of relative density of 1025 kg/m³ and the lightweight of the ship. The displacement is given in Table 2. To estimate the lightweight of the KCS container ship, Sen and Yang (2012)'s method is introduced.

Regarding efficiency coefficients, Seo et al. (2010) investigated the  $\eta_0$  of the KCS container ship. The result and collected literature data show that the value of  $\eta_0$  is between 0.613 and 0.682. The average of these results is used as the estimated value of  $\eta_0$ , which equals 0.646. According to 2.3.2,  $\eta_R$ ,  $\eta_S$ , and  $\eta_H$  are 1.0,0.98, and 1.08 respectively. The main parameters of the main engine and auxiliary engine are listed in Table 3, including the fuel type used in this case and the corresponding SFOC and  $C_F$  (Kristensen, 2017). The price of fuel oil is assumed to be 550 US dollars.

The reduction factor Z of CII calculation is 7, according to the regulatory standards for 2024.

#### 3.1.1. The trans-Indian Ocean route

A trans-Indian Ocean route from Gqeberha to Banda Aceh, as illustrated in Fig. 7, is introduced as the target route. The vessel is assumed to be fully loaded throughout the whole navigation, regardless of other operational elements. The ship, in this case, is set to depart from Gqeberha at 00:00 on April 22, 2024. In this case, the sailing time is represented as hours starting from 00:00 on April 22, 2024, such as t=0 represents 00:00/22/4/2024 and t=48 means 00:00/24/4/2024. It has to be noted that the target navigation area is divided into a grid of cells of 0.25 longitude by 0.25 dimension to align the data from Deutscher Wetterdienst (DWD) (Wetterdienst). The wave height, wave period, wave direction, wind velocity, and wind direction data from DWD are given for each cell. Based on these input data, the CCPC, carbon emission, and other results of each cell could be acquired, which are used to evaluate and optimize shipping routes.

#### 3.1.2. The liner route between Shanghai and Busan

The round trip diagram of the liner traveling service between Shanghai and Busan is illustrated in Fig. 7. The route is not only a conventional intra-Asia route but also an important component of trans-Pacific routes according to shipping service provider (OOCL). The vessel is assumed to be fully loaded throughout the whole navigation regardless of other operational elements. Conventionally, the schedule of liner service is made in advance. Herein, the shipping schedule is set for two round-trip sailings over eight days considering that the short-term forecast period of marine weather is about one week. The ship in this case is set to depart from Shanghai at 00:00 on December 4, 2023. After arriving in Busan and completing the unloading and loading work, the ship is set to leave the port for Shanghai at 00:00 on December 6, 2023. This round trip would be repeated and the next departure time of Shanghai and Busan are 00:00 on December 8, 2023 and 00:00 on December 10, 2023 respectively. In this case, the sailing time is represented as hours starting from 00:00 on December 4, 2023, such as t = 0 represents 00:00/4/12/2023 and t = 48 means 00:00/6/12/2023.

#### 3.2. Experiments of trans-Indian Ocean route

# 3.2.1. Tracking of CCPC

The results of the entire voyage from Gqeberha to Banda Aceh based on three ship routing methods are illustrated in Fig. 8. As shown in the chart, the *Attained CII* based on the developed framework and CCPC are monitored throughout the entire navigation. The curve of *Attained CII* (black line) represents *Real-time CII* derived by Eq. (4), which reflects the real-time energy efficiency level of the ship and is constantly changing due to operating conditions and sea states. The presented curve of *Attained CII* is drawn using the mean value

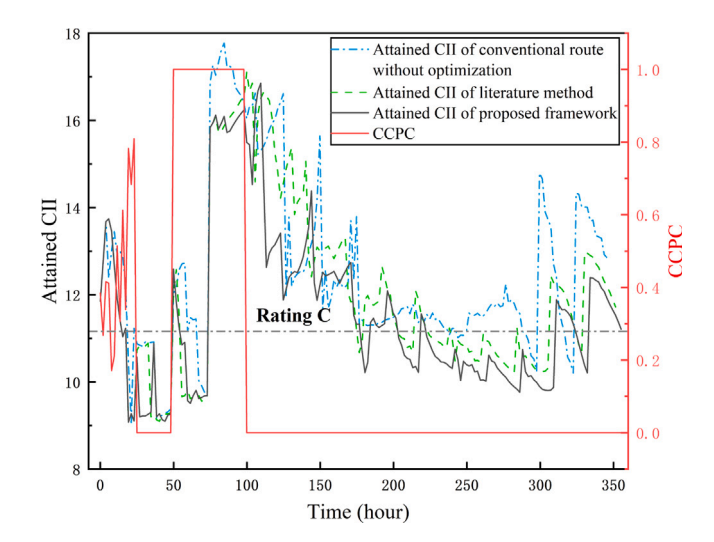


Fig. 8. The real-time CCPC and Attained CII during trans-India Ocean navigation based on proposed framework, literature method (Wei et al., 2023), and conventional route.

of predicted Attained CII. As encountering severe sea conditions, the Attained CII curve is above and below rating C 52.15% and 47.85% of the total sailing time, respectively. As shown in Fig. 8, the proposed ship routing framework implements the full range prediction of CCPC, which reveals the compliance level of CII at any time during the voyage. In this calculation, the historical carbon emissions  $M_h$  and historical transport work  $W_h$  are set as 0, which is equivalent to shipping conditions at the beginning of each calendar year according to regulations of CII. The initial CCPC is at a low level(less than 0.4), which means the ship encountered relatively rough sea conditions when it departs from Ggeberha. Subsequently, CCPC is immediately improved due to optimized routes. Then, it could be found that CCPC decreases to 0 before t = 50 even though the value of Attained CII is lower than rating C during this period. This is caused by previously accumulated carbon emissions. This phenomenon is also reflected in the subsequent jumps in the CCPC curve. From the perspective of the entire voyage, the CCPC performance of the ship was poor due to the severe sea conditions encountered during the voyage. It has to be pointed out that the jumps of the CCPC curve are caused by the time resolution of ocean weather data, and the time resolution in this section is 24 h. Hence, in every 24 h of ship routing, the prediction of CCPC at each moment could only use previous data.

A ship routing method, only Attained CII concerned for optimization, in the literature (Wei et al., 2023) is introduced as a comparison. The results of Attained CII derived by the literature method are drawn as the green dotted line in Fig. 8. The mean value of Attained CII and time of rating C for the literature method are 12.09 and 42.93%. It could be found that the Attained CII of the proposed framework is lower than the Attained CII of literature method 73.91% sailing time. Compared with the literature method, the proposed framework reduces Attained CII by about 4.14% and increases the time of rating C by about 4.92%. This suggests that the proposed framework further enhances decarbonization capabilities and improves compliance performance for ship routing. It has to be noted that the sharp peaks of the black and green lines are caused by the update of ocean data or departure and arrival. It results in locations that were ideal in the previous ocean data becoming more severe in the updated data, and there is no time to evade. This issue could be improved by increasing the time resolution of ocean data.

In addition, a conventional route without optimization is introduced in this case to compare with the proposed framework. The conventional route means sailing directly from the departure port to the destination port without deviation or adjustment due to environmental factors.

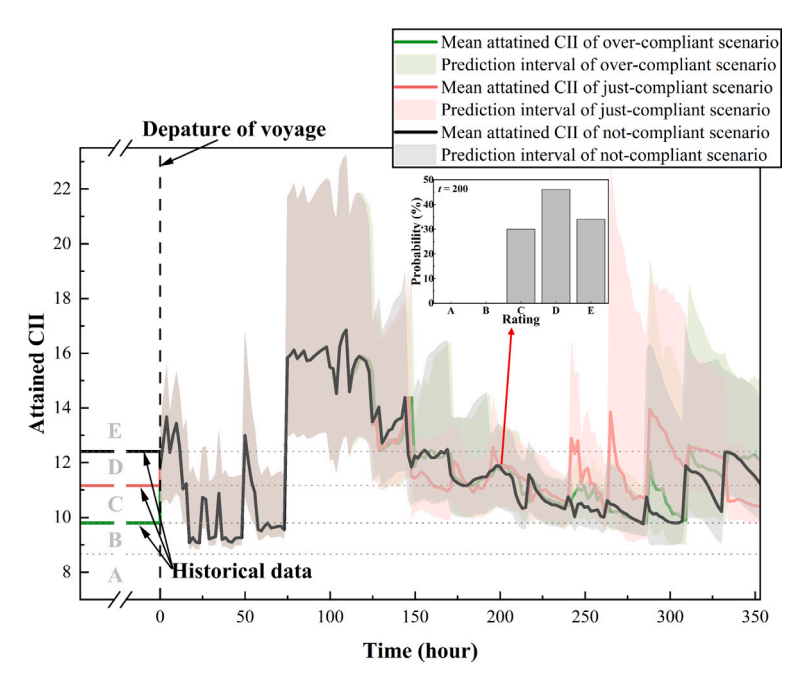


Fig. 9. Prediction interval of Attained CII under three compliant scenarios and probability results of CII rating forecast.

This is feasible in this case because the ports of Gqeberha and Banda Aceh are separated only by the Indian Ocean. This is also in line with the general ship navigation operation practice according to the ship AIS track charts publicly available on the Internet. The Attained CII of the conventional route is presented in Fig. 8 as the blue line. Despite the conventional route shortening the navigation time by 10.4 h, its Attained CII increases significantly throughout the navigation compared with the proposed framework. For 77.9% of the sailing time, the decarbonization performance of the conventional route is worse than the route of the proposed framework, i.e., the blue line is above the black line. The mean values of Attained CII for the conventional route and proposed route are 12.54 and 11.59, respectively. Compared with the conventional route, the proposed route increases voyage time by 3.04% but reduces Attained CII by 7.58%. This reflects the feasibility and effectiveness of the proposed framework to enhance the decarbonization performance of ships by sacrificing a certain amount of sailing time.

# 3.2.2. Results based on different historical states

The historical carbon emission and transport work are set as 0 in Section 3.2.1. It only corresponds to the shipping conditions at the beginning of each year. Three different shipping scenarios are investigated in this section: over-compliant, just-compliant, and not-compliant. Herein, the ship is assumed to have sailed 31,500 nautical miles fully loaded from the beginning of the year till this task (i.e., time equals 0 in Fig. 9). The assumptions of sailing distance and load are utilized to calculate the historical carbon emission and transport work of three typical shipping scenarios. It has to be noticed that speed and navigation time are not considered in the assumptions of historical data as *Attained CII* is only determined by the weight of carbon emission and transport work as presented in Eq. (1).

The over-compliant scenario represents that the historical CII rating is superior to rating C. The results of the over-compliant scenario are shown in Fig. 9. The historical *Attained CII* is assumed as 9.8 g/t·n miles corresponds to 12,736 tons  $CO_2$  and  $1.3 \times 10^9$  t·n miles. According to Fig. 9, the energy efficiency level and compliance performance of the ship could be intuitively revealed. The distribution probability of the real-time CII rating could be derived as illustrated in the sub-graph of Fig. 9. At the time of t=200, the probabilities of getting C, D, and E are 30%, 46%, and 34%, respectively, and the probabilities of being

rated at ratings A and B are both 0. Besides, The historical *Attained CII* of the just-compliant scenario is set to be exactly equal to the rating C standard, i.e. 11.16 g/t·n miles, and the value of historical *Attained CII* for a not-compliant scenario is set as 11.2 which is larger than the rating C standard.

The optimized routes of three scenarios are drawn in Fig. 10. The background of the picture uses the wave height data at 00:00 on April 28. The 'Route of rating B/C/D' corresponds to the over-compliant scenario, just-compliant scenario, and not-compliant scenario, respectively. It could be found that 'Route of rating B' has the smallest deviation compared to the other two routes as it has better historical data on CII compliance. The 'Route of rating C' and 'Route of rating D' have more deviations and detours compared with the 'Route of rating B'. This is because the historical Attained CII is not less than the rating C standard, and the developed framework would search for a path with better compliance performance under the supervision of rating C. The developed ship routing framework optimizes routes based on CCPC to improve the performance of shipping compliance. The degree and speed of the improvement are affected by historical shipping distance. As sailing distances increase, it becomes increasingly difficult to improve regulatory compliance through ship routing.

# 3.2.3. Results based on time preference

As expressed in Section 2.5, the impact of the time preference on the proposed ship routing framework will be investigated separately in this section. Considering the regulatory requirements of CII expressed in Section 2.5, the time preference of ship stakeholders depends on the choice of rating sequence over three years or longer. To describe stakeholders' time preference in short-term ship routing within one year, the time preference herein is set as selecting rating C or D for supervision standard, i.e., selecting rating C represents that stakeholders prefer long-term benefits, and selecting rating D means the opposite. It has to be noted that the time preference in this section is not standard probability discounting because future benefits are not concerned. Herein, time preference is introduced to reflect the decision-maker's short-term preferences within one year.

The calculated results are listed in Table 4, and two routes are drawn in Fig. 11. The route of C means long-term return preference, and the route of D represents the short-term. It can be found that the route of rating D decreases shipping cost by about 2.3% compared with

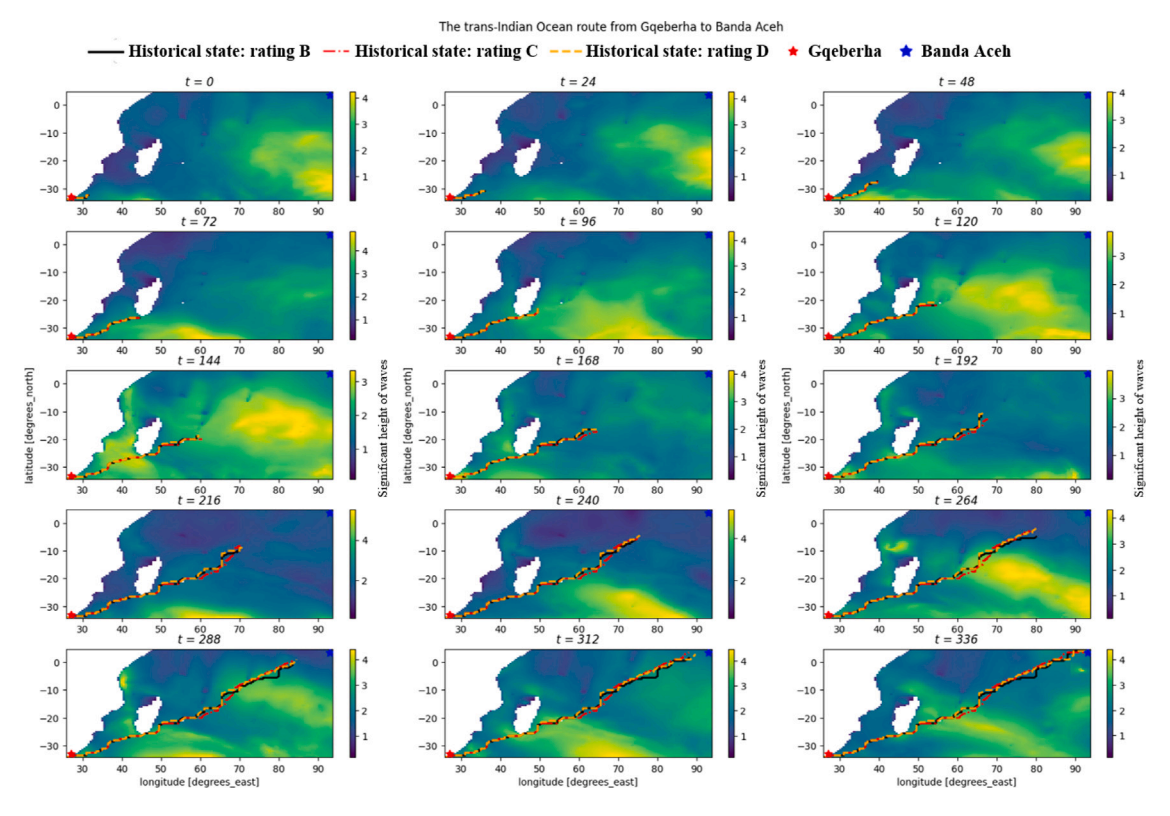


Fig. 10. Optimized routes of trans-India Ocean navigation based on three scenarios. The curves of routes in the figure are Gaussian fitting and smoothing.

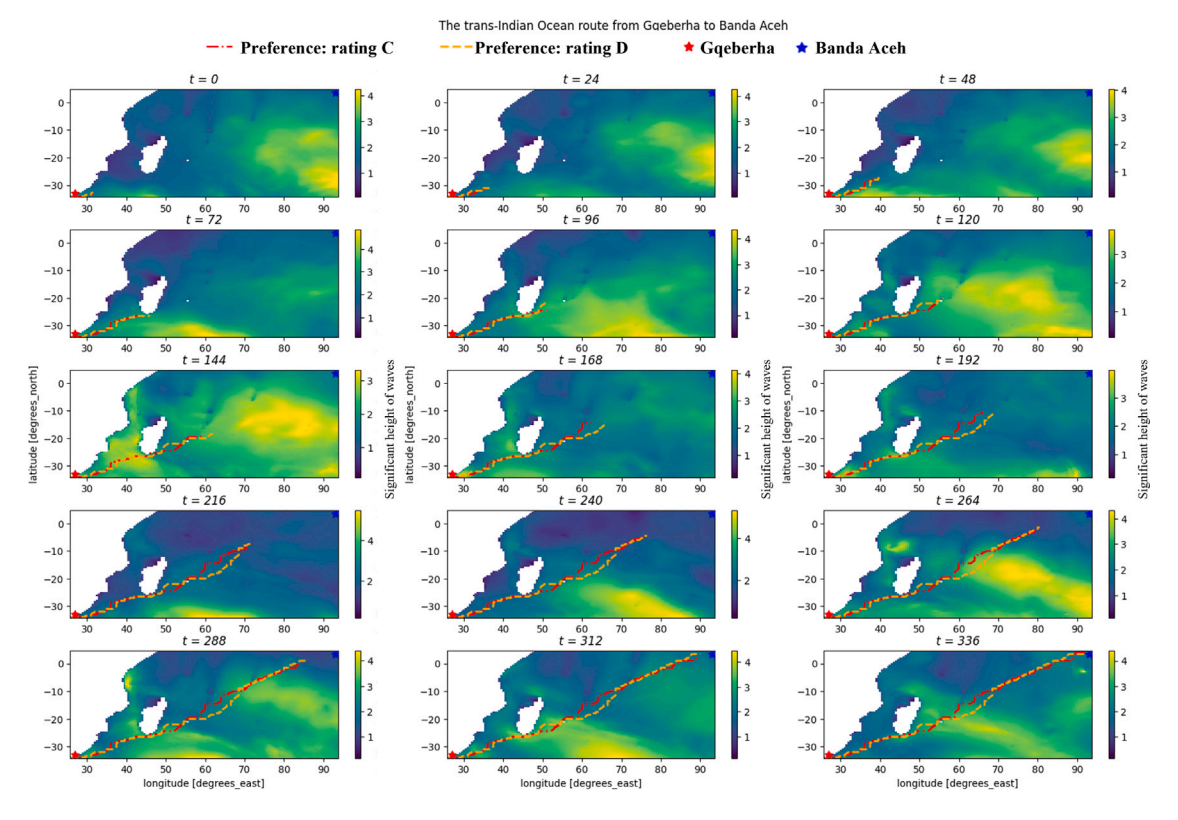


Fig. 11. The comparison diagram of routes derived based on different rating standards. The curves of routes in the figure are Gaussian fitting and smoothing. For ease of presentation and reading, wave height during the voyage is chosen as the picture background rather than multi-wave properties at different moments of the voyage.

Table 4
Main results of ship routing based on diverse time preference.

Rating of standard	Sailing distance [n mile]	Sailing time [hour]	Mean value of Attained CII [g/ton nmile]	Mean value of CO <sub>2</sub> emission [ton]	Cost [USD]
С	4617.6	355.2	11.59	2223.3	1 785 849
D	4568.2	351.4	11.98	2273.7	1779631

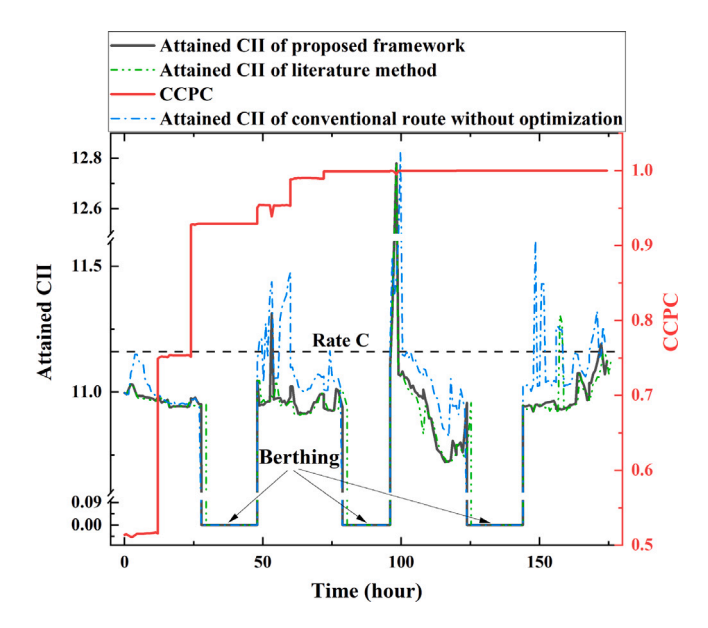


Fig. 12. The real-time CCPC and Attained CII during liner navigation based on proposed framework, literature method (Wei et al., 2023), and conventional route.

the route of rating C. Meanwhile, the mean value of *Attained CII* of D-route rises about 3.4%. As shown in Fig. 11, the route of rating D has fewer deviations and detours compared with the other route, which leads to a drop in shipping cost. From a short-term perspective, the benefits of choosing the time preference based on rating D are significant. However, the long-term return could be affected by the burgeoning regulations. Hence, current time preference should be determined based on a life cycle operating plan such as significant retrofits and operational strategy adjustment.

# 3.3. Experiments of liner route between shanghai and busan

# 3.3.1. Tracking of CCPC

The CCPC of the round shipping route is tracked in the same way as presented in 3.2.1. The historical carbon emissions  $M_h$  and historical transport work  $W_h$  are set as 0 as same as Section 3.2.1. The initial CCPC is at a medium level due to the upper boundary of predicted Attained CII being higher than the rate C standard. The CCPC increases and stabilizes at 1 with the Attained CII consistently less than the rate C standard. It has to be noted that the three horizontal line segments at the bottom represent the time of unloading and loading in two ports. The carbon emissions during this period are assumed to be 0 considering that vessels can use shore power and other methods to cut carbon emissions onboard.

It can be found that even the wave and wind conditions in East China sea are much weaker than those in the Indian Ocean (Zheng et al., 2022). The proposed framework is still able to seize the opportunity to reduce emissions and Attained CII. As shown in Fig. 12, compared with the conventional route, i.e. straight sailing, Attained CII of the optimized route decreases by 1.2% on average. The literature (Wei et al., 2023) is also introduced in this navigation for comparison. The results of Attained CII derived by the literature method are drawn as the green dotted line in Fig. 12. During the overlapping sailing time,

it can be seen that the green dotted line is below or overlapping the black line most of the time, i.e. about 75% sailing time. The mean values of *Attained CII* derived by the proposed framework and the literature approach are 10.98 [g/ton · n mile] and 10.96 [g/ton · n mile] respectively. The mean value of *Attained CII* increases by less than 0.2% but the proposed framework saves about 5% of the shipping cost. The cost reduction derived from the shorter sailing distance and time which means less deviation and detour during the voyage. By multicriteria optimization, the proposed framework reduces the shipping cost effectively with a minor increase of *Attained CII* within regulatory limits. Compared with literature methods, the proposed approach has better performance in balancing decarbonization indicators and shipping costs.

# 3.3.2. Results based on different historical states

The historical carbon emission and transport work are set as same as settings in 3.2.2. Herein, three shipping scenarios are also set up like 3.2.2: over-compliant, just-compliant, and not-compliant.

The optimized routes on a round trip voyage of three scenarios are drawn in Fig. 13. The 'Route of rate B/C/D' corresponds to the over-compliant scenario, just-compliant scenario, and not-compliant scenario respectively. It can be found that the 'Route of rate C' and 'Route of rate D' are completely overlapped. This is because the historical *Attained CII* is not less than the rate C standard and the developed framework would search path with better compliance performance under the supervision of rate C. Hence, the overlapped route has more deviations and detours compared with the 'Route of rate B'. The 'Route of rate B' is closer to the general route as it has better historical data on CII compliance and it can take more cost considerations into account. In this case, the 'Route of rate B' saves about 1.3% of the cost compared to other routes.

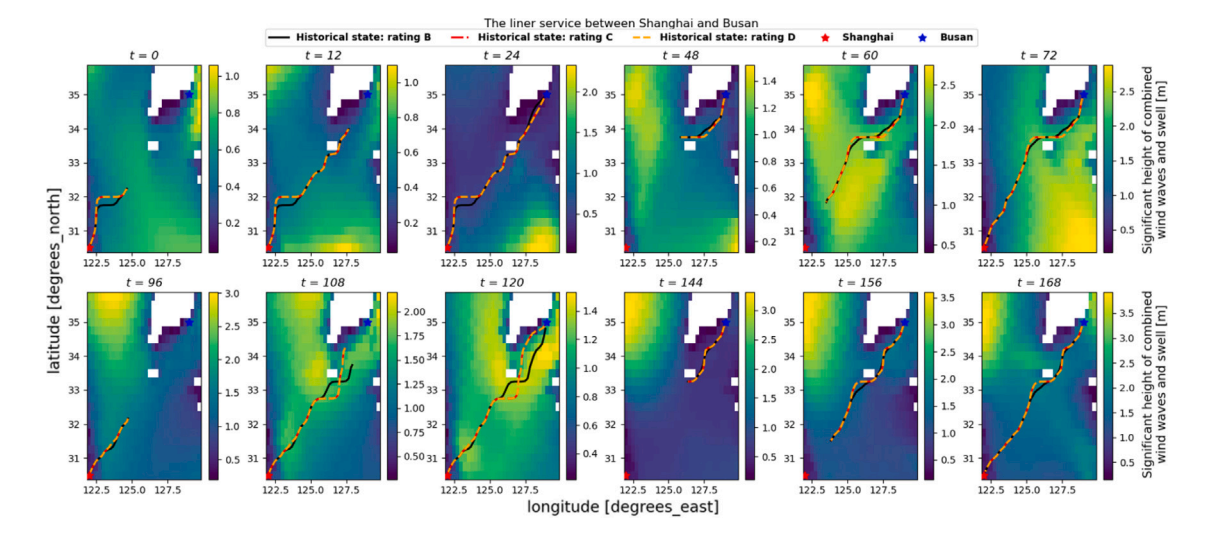


Fig. 13. Optimized routes of liner service navigation based on three scenarios. The curves of routes in the figure are Gaussian fitting and smoothing. For ease of presentation and reading, wave height during the voyage is chosen as the picture background rather than multi wave properties at different moments of the voyage.

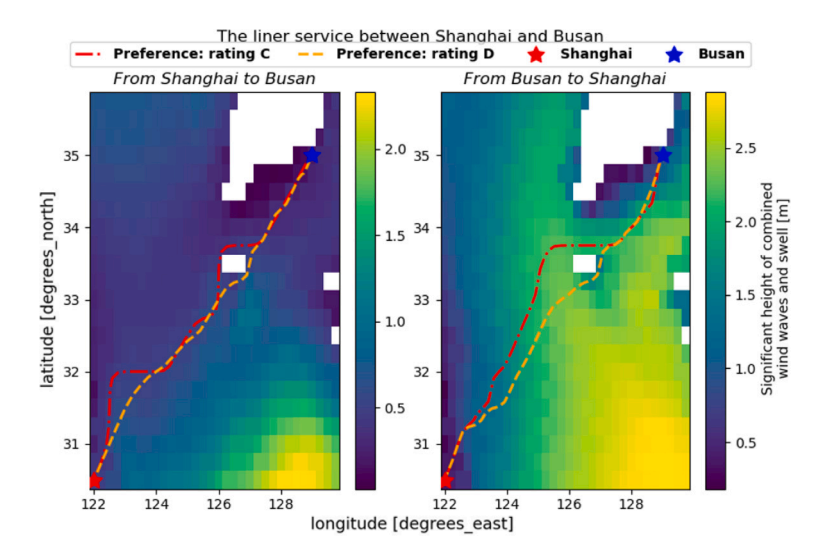


Fig. 14. The comparison diagram of routes derived based on different rating standards for liner service between Shanghai and Busan. The curves of routes in the figure are Gaussian fitting and smoothing. For ease of presentation and reading, the wave height data from the last optimization of routes are set as the background.

# 3.3.3. Results based on time preference

The settings, herein, are the same as in 3.2.3. The two routes of single round trip are drawn in Fig. 14. It can be found that the route of rating D has fewer deviations and detours compared with the route of rating C which leads to a drop in shipping cost, that is, 10% lower than route of rating C. Correspondingly, the *Attained CII* also increases from 10.97 in route of rating C to 11.98 in route of rating D, i.e., an increase of 9.2%. In this liner service route, cost can be adjusted by changing time preferences based on the proposed framework.

#### 4. Conclusions

This study established a ship routing framework based on a novel indicator(i.e., CCPC) to improve vessels' ability to cope with the supervision of CII regulations. Wave and wind data are introduced to estimate carbon emissions and further support ship routing. The developed framework could track real-time CCPC and predict the probability of CII rating at any time during the voyage. Preferences are introduced into the proposed framework to support stakeholders' decisions concerning the balance between decarbonization compliance and cost.

With historical data merged, the ship routing framework provides results based on long-term perspectives, and the initiatives for decarbonization management of CII are enhanced. Two multi-aspect case studies are conducted to verify the effectiveness and applicability of the proposed ship routing framework.

The following conclusions are drawn:

- The proposed ship routing framework is able to enhance vessels'
  decarbonization compliance by revealing the probability of CII
  rating in time, which could provide real-time decision-making
  support for shipping operations. The impacts of ship routing
  on CII rating are gradual after a period of shipping operation.
  Constant monitoring of CII rating is beneficial for stakeholders
  to deal with the supervision of CII.
- The proposed ship routing framework could enhance vessels' decarbonization compliance with a CII rating maintained compared with the conventional approach. The rating mechanism of CII is different from past indicators. The extent of the Attained CII among a single CII rating is flexible for ship operations. The flexibility is seized in this study as an opportunity to reduce cost

**Table A.1**Normalized results of all intervals for heading = 180 deg.

Interval	Alpha	Beta	Cauchy	Gamma	d-gamma	Normal	log-normal	$\mathcal{X}^2$	Weibull	e-weibull	d-weibull
0.1-0.3	0.56	0.00	1.28	0.70	0.56	0.51	0.53	0.89	3.00	0.74	0.40
0.3-0.5	1.21	0.69	1.35	0.97	1.64	0.95	2.10	0.43	0.60	0.73	1.36
0.5-0.7	1.20	0.00	2.82	1.17	1.49	1.13	1.18	2.42	1.00	0.99	1.30
0.7-0.9	0.98	0.00	2.86	1.33	1.94	1.11	0.86	0.80	0.56	1.27	1.45
0.9 - 1.1	0.90	1.00	2.63	0.85	1.03	0.89	0.86	0.85	0.78	1.01	0.97
1.1-1.3	1.63	0.52	3.00	1.50	1.74	1.34	1.45	1.54	1.00	0.26	1.58
1.3-1.5	0.34	0.04	1.95	0.35	0.83	0.32	0.36	3.00	0.18	0.02	0.77
1.5-1.7	1.29	0.00	1.18	3.00	0.83	0.59	0.71	0.84	2.42	1.50	0.80
1.7-1.9	1.39	0.61	2.51	1.35	1.46	1.28	1.33	2.26	1.23	0.88	1.59
1.9-2.1	2.95	0.00	2.72	1.03	1.44	0.96	1.01	1.03	1.04	0.59	1.30
2.1-2.3	1.41	0.33	1.31	1.02	1.75	1.00	2.26	0.84	1.01	1.15	0.63
2.3-2.5	1.07	0.64	1.49	1.07	1.45	1.05	1.06	1.03	1.06	2.00	1.20
SUM	14.94	3.83	25.12	14.33	16.18	11.13	13.69	15.93	13.88	11.13	13.34

Table A.2

Normalized results of each distribution fitting for each heading.

Heading	Alpha	Beta	Cauchy	Gamma	d-gamma	Normal	log-normal	$\mathcal{X}^2$	Weibull	e-weibull	d-weibull
180	14.94	3.83	25.12	14.33	16.18	11.13	13.69	15.93	13.88	11.13	13.34
150	4.61	2.94	8.36	4.44	\	4.59	3.48	5.44	3.11	6.13	6.22
120	3.66	2.84	7.12	2.97	4.05	3.34	4.23	2.77	2.36	2.99	4.02
90	4.95	3.80	7.89	7.54	\	5.20	7.08	7.72	4.02	5.46	7.62
60	3.32	3.09	6.44	3.30	\	3.60	4.04	4.55	3.04	5.43	6.90
30	3.99	4.11	7.05	4.76	\	4.05	2.92	3.57	3.72	3.04	7.29
0	3.63	2.79	9.75	3.51	5.80	3.43	3.64	7.47	2.76	4.79	4.89
SUM	39.11	23.40	71.72	40.84	\	35.34	39.09	47.45	32.89	38.98	50.29

with the CII rating maintained. Two different cases are introduced to validate the applicability of the proposed framework.

The impact of preferences on compliance and costs is essential
for ship operations from both long and short-term perspectives.
The presented case studies show the influence of preferences
on ship operations, which could support the decision-making of
stakeholders. Further work has to be focused on investigating the
mechanism of preferences, especially time preference, affecting
compliance and cost.

Several limitations have to be recognized in the proposed framework. The sailing speed is implemented as a constant value in case studies. This reduces the flexibility of the framework, which cannot apply lower speed under a more stringent supervision standard. The ship routing algorithm with speed concerned is essential to enhance the flexibility of the framework in further study. This study only considers the uncertainty effects of wave added resistance and auxiliary engine power. The uncertainty of auxiliary engine power is analyzed based on public data limits its applicability outside of this dataset. However, it has to be noticed that the data could be replaced by vessels' historical data in specific scenarios to enhance applicability as the framework is modularized. The uncertainty effects of other factors, such as ship fouling, have not been included in the proposed framework. The impact of the ship's laden and ballast states on the ship's energy efficiency and CII is not discussed as the ship in case studies is set to be fully loaded. Further research into laden and ballast conditions could enable optimization of costs and decarbonization performance over the vessels' life cycle. Low time and space resolution are limitations of the proposed framework. Higher resolution accuracy could help improve the effectiveness of the framework.

# CRediT authorship contribution statement

**Qikun Wei:** Writing – original draft, Methodology, Conceptualization, Software, Formal analysis. **Yan Liu:** Methodology, Writing – review & editing, Funding acquisition. **You Dong:** Methodology, Validation. **Meixia Chen:** Supervision, Validation.

#### Declaration of competing interest

The authors declare that they have no known competing financial interests or personal relationships that could have appeared to influence the work reported in this paper.

#### Acknowledgments

This work was supported by the National Natural Science Foundation of China (Grant No. 52471327), the State Key Laboratory of Ocean Engineering (Shanghai Jiao Tong University), China (Grant No. GKZD010084), and the Interdisciplinary Research Program of HUST (Grant No. 2024JCYJ029).

# Appendix. Results of uncertainty analysis for wave added resistance

This appendix presents the basic procedure and calculation results for obtaining the optimum distribution of added wave resistance as an explanation and supplement to the part *Uncertainty of main engine power* in Section 2.3.3.

In Table A.1, each row is the sum of the normalized SSE, AIC, and BIC in the selected interval. The values of each interval are summed to get the last row of the table. For the last row, the smaller the Sum value, the better the fit of the distribution. Based on the results of Table A.1, it can be determined that the beta distribution is the most appropriate probability distribution for heading = 180 degrees.

The same analysis process is conducted on all seven headings, i.e.,  $180,\,150,\,120,\,90,\,60,\,30,\,$  and 0 degrees. The detailed results are presented in Table A.3.

Furthermore, Table A.2 presents the results of the goodness-of-fit analysis (the sum value in Table A.3) for the response distributions corresponding to the seven headings.

After determining the introduction of the beta distribution, the coefficients of the beta distribution were determined and listed in Table A.4. These parameters would determine a specific beta distribution for  $C_{\rm AW}$  under different scenarios.

 $\mbox{\bf Table A.3} \\ \mbox{Normalized results of $C_{\rm AW}$ fitted distributions for each intervals for all headings.}$ 

180 deg  0.1–0.3	1.19 0.00 0.00 1.03 0.73 2.94 0.42 0.52 1.89	1.28 1.35 2.82 2.86 2.63 3.00 1.95 1.18 2.51 2.72 1.31 1.49 25.12  2.45 1.22 3.00 0.76 0.93 8.36	0.70 0.97 1.17 1.33 0.85 1.50 0.35 3.00 1.35 1.03 1.02 1.07 14.33	0.56 1.64 1.49 1.94 1.03 1.74 0.83 0.83 1.46 1.44 1.75 1.45 16.18	0.51 0.95 1.13 1.11 0.89 1.34 0.32 0.59 1.28 0.96 1.00 1.05 11.13	0.53 2.10 1.18 0.86 0.86 1.45 0.36 0.71 1.33 1.01 2.26 1.06 13.69	0.89 0.43 2.42 0.80 0.85 1.54 3.00 0.84 2.26 1.03 0.84 1.03 0.84 2.26 2.19 0.92	3.00 0.60 1.00 0.56 0.78 1.00 0.18 2.42 1.23 1.04 1.01 1.06 13.88	0.74 0.73 0.99 1.27 1.01 0.26 0.02 1.50 0.88 0.59 1.15 2.00 11.13	0.40 1.36 1.30 1.45 0.97 1.58 0.77 0.80 1.59 1.30 0.63 1.20 13.34
0.3-0.5 1.21 0.5-0.7 1.20 0.7-0.9 0.98 0.9-1.1 0.90 1.1-1.3 1.63 1.3-1.5 0.34 1.5-1.7 1.29 1.7-1.9 1.39 1.9-2.1 2.95 2.1-2.3 1.41 2.3-2.5 1.07 SUM 14.94 150 deg 0.1-0.5 1.27 0.5-1.0 0.49 1.0-1.5 1.24 1.5-2.0 0.66 2.0-2.5 0.96 SUM 4.61 120 deg 0.1-0.5 0.53 0.5-1.0 1.40 1.0-1.5 1.73 SUM 3.66 90 deg 0.1-0.5 0.91 0.5-1.0 0.65 1.0-1.5 1.31 1.5-2.0 0.00 2.0-2.5 2.07 SUM 4.95	0.69 0.00 0.00 1.00 0.52 0.04 0.00 0.61 0.00 0.33 0.64 3.83 1.19 0.00 0.00 1.03 0.73 2.94	1.35 2.82 2.86 2.63 3.00 1.95 1.18 2.51 2.72 1.31 1.49 25.12 2.45 1.22 3.00 0.76 0.93 8.36	0.97 1.17 1.33 0.85 1.50 0.35 3.00 1.35 1.03 1.02 1.07 14.33	1.64 1.49 1.94 1.03 1.74 0.83 0.83 1.46 1.44 1.75 1.45 16.18	0.95 1.13 1.11 0.89 1.34 0.32 0.59 1.28 0.96 1.00 1.05 11.13  1.00 0.44 1.20 0.99 0.96	2.10 1.18 0.86 0.86 1.45 0.36 0.71 1.33 1.01 2.26 1.06 13.69	0.43 2.42 0.80 0.85 1.54 3.00 0.84 2.26 1.03 0.84 1.03 15.93	0.60 1.00 0.56 0.78 1.00 0.18 2.42 1.23 1.04 1.01 1.06 13.88	0.73 0.99 1.27 1.01 0.26 0.02 1.50 0.88 0.59 1.15 2.00 11.13	1.36 1.30 1.45 0.97 1.58 0.77 0.80 1.59 1.30 0.63 1.20 13.34
0.3-0.5 1.21 0.5-0.7 1.20 0.7-0.9 0.98 0.9-1.1 0.90 1.1-1.3 1.63 1.3-1.5 0.34 1.5-1.7 1.29 1.7-1.9 1.39 1.9-2.1 2.95 2.1-2.3 1.41 2.3-2.5 1.07 SUM 14.94 150 deg 0.1-0.5 1.27 0.5-1.0 0.49 1.0-1.5 1.24 1.5-2.0 0.66 2.0-2.5 0.96 SUM 4.61 120 deg 0.1-0.5 0.53 0.5-1.0 1.40 1.0-1.5 1.73 SUM 3.66 90 deg 0.1-0.5 0.91 0.5-1.0 0.65 1.0-1.5 1.31 1.5-2.0 0.00 2.0-2.5 2.07 SUM 4.95	0.00 0.00 1.00 0.52 0.04 0.00 0.61 0.00 0.33 0.64 3.83 1.19 0.00 0.00 1.03 0.73 2.94	1.35 2.82 2.86 2.63 3.00 1.95 1.18 2.51 2.72 1.31 1.49 25.12 2.45 1.22 3.00 0.76 0.93 8.36	1.17 1.33 0.85 1.50 0.35 3.00 1.35 1.03 1.02 1.07 14.33	1.49 1.94 1.03 1.74 0.83 0.83 1.46 1.44 1.75 1.45 16.18	1.13 1.11 0.89 1.34 0.32 0.59 1.28 0.96 1.00 1.05 11.13	1.18 0.86 0.86 1.45 0.36 0.71 1.33 1.01 2.26 1.06 13.69	2.42 0.80 0.85 1.54 3.00 0.84 2.26 1.03 0.84 1.03 15.93	1.00 0.56 0.78 1.00 0.18 2.42 1.23 1.04 1.01 1.06 13.88	0.99 1.27 1.01 0.26 0.02 1.50 0.88 0.59 1.15 2.00 11.13	1.30 1.45 0.97 1.58 0.77 0.80 1.59 1.30 0.63 1.20 13.34
0.7-0.9 0.98 0.9-1.1 0.90 1.1-1.3 1.63 1.3-1.5 0.34 1.5-1.7 1.29 1.7-1.9 1.39 1.9-2.1 2.95 2.1-2.3 1.41 2.3-2.5 1.07 SUM 14.94 150 deg 0.1-0.5 1.27 0.5-1.0 0.49 1.0-1.5 1.24 1.5-2.0 0.66 2.0-2.5 0.96 SUM 4.61 120 deg 0.1-0.5 0.53 0.5-1.0 1.40 1.0-1.5 1.73 SUM 3.66 90 deg 0.1-0.5 0.91 0.1-0.5 0.91 0.5-1.0 0.65 1.0-1.5 1.31 1.5-2.0 0.00 2.0-2.5 2.07 SUM 4.95	0.00 1.00 0.52 0.04 0.00 0.61 0.00 0.33 0.64 3.83 1.19 0.00 0.00 1.03 0.73 2.94 0.42 0.52 1.89	2.86 2.63 3.00 1.95 1.18 2.51 2.72 1.31 1.49 25.12 2.45 1.22 3.00 0.76 0.93 8.36	1.33 0.85 1.50 0.35 3.00 1.35 1.02 1.07 14.33 1.18 0.47 1.24 0.59 0.96 4.44	1.94 1.03 1.74 0.83 0.83 1.46 1.44 1.75 1.45 16.18	1.11 0.89 1.34 0.32 0.59 1.28 0.96 1.00 1.05 11.13	0.86 0.86 1.45 0.36 0.71 1.33 1.01 2.26 1.06 13.69	0.80 0.85 1.54 3.00 0.84 1.03 15.93 0.98 0.92 2.19	0.56 0.78 1.00 0.18 2.42 1.23 1.04 1.01 1.06 13.88	1.27 1.01 0.26 0.02 1.50 0.88 0.59 1.15 2.00 11.13	1.45 0.97 1.58 0.77 0.80 1.59 1.30 0.63 1.20 13.34
0.9-1.1         0.90           1.1-1.3         1.63           1.3-1.5         0.34           1.5-1.7         1.29           1.7-1.9         1.39           1.9-2.1         2.95           2.1-2.3         1.41           2.3-2.5         1.07           SUM         14.94           150 deg         1.27           0.5-1.0         0.49           1.0-1.5         1.24           1.5-2.0         0.66           2.0-2.5         0.96           SUM         4.61           120 deg         0.1-0.5           0.5-1.0         1.40           1.0-1.5         1.73           SUM         3.66           90 deg         0.1-0.5           0.5-1.0         0.65           1.0-1.5         1.31           1.5-2.0         0.00           2.0-2.5         2.07           SUM         4.95	1.00 0.52 0.04 0.00 0.61 0.00 0.33 0.64 3.83 1.19 0.00 0.00 1.03 0.73 2.94 0.42 0.52 1.89	2.63 3.00 1.95 1.18 2.51 2.72 1.31 1.49 25.12 2.45 1.22 3.00 0.76 0.93 8.36	0.85 1.50 0.35 3.00 1.35 1.02 1.07 14.33 1.18 0.47 1.24 0.59 0.96 4.44	1.03 1.74 0.83 0.83 1.46 1.44 1.75 1.45 16.18	0.89 1.34 0.32 0.59 1.28 0.96 1.00 1.05 11.13	0.86 0.86 1.45 0.36 0.71 1.33 1.01 2.26 1.06 13.69	0.85 1.54 3.00 0.84 2.26 1.03 0.84 1.03 15.93	0.78 1.00 0.18 2.42 1.23 1.04 1.01 1.06 13.88	1.01 0.26 0.02 1.50 0.88 0.59 1.15 2.00 11.13	0.97 1.58 0.77 0.80 1.59 1.30 0.63 1.20 13.34
1.1–1.3 1.63 1.3–1.5 0.34 1.5–1.7 1.29 1.7–1.9 1.39 1.9–2.1 2.95 2.1–2.3 1.41 2.3–2.5 1.07 SUM 14.94 150 deg  0.1–0.5 1.27 0.5–1.0 0.49 1.0–1.5 1.24 1.5–2.0 0.66 2.0–2.5 0.96 SUM 4.61 120 deg  0.1–0.5 0.53 0.5–1.0 1.40 3.66 90 deg  0.1–0.5 0.91 0.5–1.0 0.65 1.0–1.5 1.31 1.5–2.0 0.00 2.0–2.5 2.07 SUM 4.95	0.52 0.04 0.00 0.61 0.00 0.33 0.64 3.83 1.19 0.00 0.00 1.03 0.73 2.94 0.42 0.52 1.89	3.00 1.95 1.18 2.51 2.72 1.31 1.49 25.12 2.45 1.22 3.00 0.76 0.93 8.36	0.85 1.50 0.35 3.00 1.35 1.02 1.07 14.33 1.18 0.47 1.24 0.59 0.96 4.44	1.74 0.83 0.83 1.46 1.44 1.75 1.45 16.18	1.34 0.32 0.59 1.28 0.96 1.00 1.05 11.13 1.00 0.44 1.20 0.99	1.45 0.36 0.71 1.33 1.01 2.26 1.06 13.69	1.54 3.00 0.84 2.26 1.03 0.84 1.03 15.93	1.00 0.18 2.42 1.23 1.04 1.01 1.06 13.88	0.26 0.02 1.50 0.88 0.59 1.15 2.00 11.13	1.58 0.77 0.80 1.59 1.30 0.63 1.20 13.34
1.3-1.5	0.04 0.00 0.61 0.00 0.33 0.64 3.83 1.19 0.00 0.00 1.03 0.73 2.94 0.42 0.52 1.89	1.95 1.18 2.51 2.72 1.31 1.49 25.12 2.45 1.22 3.00 0.76 0.93 8.36	0.35 3.00 1.35 1.03 1.02 1.07 14.33 1.18 0.47 1.24 0.59 0.96 4.44	0.83 0.83 1.46 1.44 1.75 1.45 16.18	0.32 0.59 1.28 0.96 1.00 1.05 11.13 1.00 0.44 1.20 0.99	0.36 0.71 1.33 1.01 2.26 1.06 13.69	3.00 0.84 2.26 1.03 0.84 1.03 15.93 0.98 0.92 2.19	0.18 2.42 1.23 1.04 1.01 1.06 13.88	0.02 1.50 0.88 0.59 1.15 2.00 11.13	0.77 0.80 1.59 1.30 0.63 1.20 13.34
1.3-1.5	0.04 0.00 0.61 0.00 0.33 0.64 3.83 1.19 0.00 0.00 1.03 0.73 2.94 0.42 0.52 1.89	1.95 1.18 2.51 2.72 1.31 1.49 25.12 2.45 1.22 3.00 0.76 0.93 8.36	0.35 3.00 1.35 1.03 1.02 1.07 14.33 1.18 0.47 1.24 0.59 0.96 4.44	0.83 0.83 1.46 1.44 1.75 1.45 16.18	0.32 0.59 1.28 0.96 1.00 1.05 11.13 1.00 0.44 1.20 0.99	0.36 0.71 1.33 1.01 2.26 1.06 13.69	3.00 0.84 2.26 1.03 0.84 1.03 15.93 0.98 0.92 2.19	0.18 2.42 1.23 1.04 1.01 1.06 13.88	0.02 1.50 0.88 0.59 1.15 2.00 11.13	0.77 0.80 1.59 1.30 0.63 1.20 13.34
1.7-1.9 1.39 1.9-2.1 2.95 2.1-2.3 1.41 2.3-2.5 1.07 SUM 14.94 150 deg 0.1-0.5 1.27 0.5-1.0 0.49 1.0-1.5 1.24 1.5-2.0 0.66 2.0-2.5 0.96 SUM 4.61 120 deg 0.1-0.5 0.53 0.5-1.0 1.40 1.0-1.5 1.73 SUM 3.66 90 deg 0.1-0.5 0.91 0.5-1.0 0.65 1.0-1.5 1.31 1.5-2.0 0.00 2.0-2.5 2.07 SUM 4.95	0.61 0.00 0.33 0.64 3.83 1.19 0.00 0.00 1.03 0.73 2.94 0.42 0.52 1.89	2.51 2.72 1.31 1.49 25.12 2.45 1.22 3.00 0.76 0.93 8.36	1.35 1.03 1.02 1.07 14.33 1.18 0.47 1.24 0.59 0.96 4.44	1.46 1.44 1.75 1.45 16.18 1.29 0.67 1.76	1.28 0.96 1.00 1.05 11.13 1.00 0.44 1.20 0.99 0.96	1.33 1.01 2.26 1.06 13.69 1.04 0.47 1.22 0.76	2.26 1.03 0.84 1.03 15.93 0.98 0.92 2.19	1.23 1.04 1.01 1.06 13.88 0.81 0.41 1.01	0.88 0.59 1.15 2.00 11.13 0.69 3.00 0.98	1.59 1.30 0.63 1.20 13.34 1.15 0.45
1.9-2.1 2.95 2.1-2.3 1.41 2.3-2.5 1.07 SUM 14.94 150 deg 0.1-0.5 0.49 1.0-1.5 1.24 1.5-2.0 0.66 SUM 4.61 120 deg 0.1-0.5 0.53 0.5-1.0 1.40 1.0-1.5 1.73 SUM 3.66 90 deg 0.1-0.5 0.91 0.5-1.0 0.65 1.0-1.5 1.31 1.5-2.0 0.00 2.0-2.5 2.07 SUM 4.95	0.00 0.33 0.64 3.83 1.19 0.00 0.00 1.03 0.73 2.94 0.42 0.52 1.89	2.72 1.31 1.49 25.12 2.45 1.22 3.00 0.76 0.93 8.36	1.03 1.02 1.07 14.33 1.18 0.47 1.24 0.59 0.96 4.44	1.44 1.75 1.45 16.18 1.29 0.67 1.76	0.96 1.00 1.05 11.13 1.00 0.44 1.20 0.99 0.96	1.01 2.26 1.06 13.69 1.04 0.47 1.22 0.76	1.03 0.84 1.03 15.93 0.98 0.92 2.19	1.04 1.01 1.06 13.88 0.81 0.41 1.01	0.59 1.15 2.00 11.13 0.69 3.00 0.98	1.30 0.63 1.20 13.34 1.15 0.45
2.1-2.3 1.41 2.3-2.5 1.07 SUM 14.94 150 deg 0.1-0.5 1.27 0.5-1.0 0.49 1.0-1.5 1.24 1.5-2.0 0.66 SUM 4.61 120 deg 0.1-0.5 0.53 0.5-1.0 1.40 1.0-1.5 1.73 SUM 3.66 90 deg 0.1-0.5 0.91 0.5-1.0 0.65 1.0-1.5 1.31 1.5-2.0 0.00 2.0-2.5 2.07 SUM 4.95	0.33 0.64 3.83 1.19 0.00 0.00 1.03 0.73 2.94 0.42 0.52 1.89	1.31 1.49 25.12 2.45 1.22 3.00 0.76 0.93 8.36	1.02 1.07 14.33 1.18 0.47 1.24 0.59 0.96 4.44	1.75 1.45 16.18 1.29 0.67 1.76	1.00 1.05 11.13 1.00 0.44 1.20 0.99 0.96	2.26 1.06 13.69 1.04 0.47 1.22 0.76	0.84 1.03 15.93 0.98 0.92 2.19	1.01 1.06 13.88 0.81 0.41 1.01	1.15 2.00 11.13 0.69 3.00 0.98	0.63 1.20 13.34 1.15 0.45
2.3-2.5 1.07 SUM 14.94 150 deg  0.1-0.5 1.27 0.5-1.0 0.49 1.0-1.5 1.24 1.5-2.0 0.66 2.0-2.5 0.96 SUM 4.61 120 deg  0.1-0.5 0.53 0.5-1.0 1.40 1.0-1.5 1.73 SUM 3.66 90 deg  0.1-0.5 0.91 0.5-1.0 0.65 1.0-1.5 1.31 1.5-2.0 0.00 2.0-2.5 2.07 SUM 4.95	0.64 3.83 1.19 0.00 0.00 1.03 0.73 2.94 0.42 0.52 1.89	1.49 25.12 2.45 1.22 3.00 0.76 0.93 8.36	1.07 14.33 1.18 0.47 1.24 0.59 0.96 4.44	1.45 16.18 1.29 0.67 1.76	1.05 11.13 1.00 0.44 1.20 0.99 0.96	1.06 13.69 1.04 0.47 1.22 0.76	1.03 15.93 0.98 0.92 2.19	1.06 13.88 0.81 0.41 1.01	2.00 11.13 0.69 3.00 0.98	1.20 13.34 1.15 0.45
SUM 14.94 150 deg 0.1-0.5 1.27 0.5-1.0 0.49 1.0-1.5 1.24 1.5-2.0 0.66 2.0-2.5 0.96 SUM 4.61 120 deg 0.1-0.5 0.53 0.5-1.0 1.40 1.0-1.5 1.73 SUM 3.66 90 deg 0.1-0.5 0.91 0.5-1.0 0.65 1.0-1.5 1.31 1.5-2.0 0.00 2.0-2.5 2.07 SUM 4.95	1.19 0.00 0.00 1.03 0.73 2.94 0.42 0.52 1.89	2.45 1.22 3.00 0.76 0.93 8.36	1.18 0.47 1.24 0.59 0.96 4.44	16.18 1.29 0.67 1.76	11.13 1.00 0.44 1.20 0.99 0.96	13.69 1.04 0.47 1.22 0.76	15.93 0.98 0.92 2.19	0.81 0.41 1.01	11.13 0.69 3.00 0.98	13.34 1.15 0.45
150 deg  0.1-0.5	1.19 0.00 0.00 1.03 0.73 2.94 0.42 0.52 1.89	2.45 1.22 3.00 0.76 0.93 8.36	1.18 0.47 1.24 0.59 0.96 4.44	1.29 0.67 1.76	1.00 0.44 1.20 0.99 0.96	1.04 0.47 1.22 0.76	0.98 0.92 2.19	0.81 0.41 1.01	0.69 3.00 0.98	1.15 0.45
0.1-0.5	0.00 0.00 1.03 0.73 2.94 0.42 0.52 1.89	1.22 3.00 0.76 0.93 8.36 2.23 3.00	0.47 1.24 0.59 0.96 4.44	0.67 1.76 \	0.44 1.20 0.99 0.96	0.47 1.22 0.76	0.92 2.19	0.41 1.01	3.00 0.98	0.45
0.5-1.0 0.49 1.0-1.5 1.24 1.5-2.0 0.66 2.0-2.5 0.96 SUM 4.61 120 deg 0.1-0.5 0.53 0.5-1.0 1.40 3.66 90 deg 0.1-0.5 0.91 0.5-1.0 0.65 1.0-1.5 1.31 1.5-2.0 0.00 2.0-2.5 2.07 SUM 4.95	0.00 0.00 1.03 0.73 2.94 0.42 0.52 1.89	1.22 3.00 0.76 0.93 8.36 2.23 3.00	0.47 1.24 0.59 0.96 4.44	0.67 1.76 \	0.44 1.20 0.99 0.96	0.47 1.22 0.76	0.92 2.19	0.41 1.01	3.00 0.98	0.45
0.5-1.0 0.49 1.0-1.5 1.24 1.5-2.0 0.66 2.0-2.5 0.96 SUM 4.61 120 deg 0.1-0.5 0.53 0.5-1.0 1.40 3.66 90 deg 0.1-0.5 0.91 0.5-1.0 0.65 1.0-1.5 1.31 1.5-2.0 0.00 2.0-2.5 2.07 SUM 4.95	0.00 0.00 1.03 0.73 2.94 0.42 0.52 1.89	1.22 3.00 0.76 0.93 8.36 2.23 3.00	0.47 1.24 0.59 0.96 4.44	0.67 1.76 \	0.44 1.20 0.99 0.96	0.47 1.22 0.76	0.92 2.19	0.41 1.01	3.00 0.98	0.45
1.0-1.5     1.24       1.5-2.0     0.66       2.0-2.5     0.96       SUM     4.61       120 deg     1.40       0.1-0.5     0.53       0.5-1.0     1.40       1.0-1.5     1.73       SUM     3.66       90 deg     0.91       0.5-1.0     0.65       1.0-1.5     1.31       1.5-2.0     0.00       2.0-2.5     2.07       SUM     4.95	0.00 1.03 0.73 2.94 0.42 0.52 1.89	3.00 0.76 0.93 8.36 2.23 3.00	1.24 0.59 0.96 4.44	1.76 \ \	1.20 0.99 0.96	1.22 0.76	2.19	1.01	0.98	
1.5-2.0     0.66       2.0-2.5     0.96       SUM     4.61       120 deg     0.53       0.5-1.0     1.40       1.0-1.5     1.73       SUM     3.66       90 deg       0.1-0.5     0.91       0.5-1.0     0.65       1.0-1.5     1.31       1.5-2.0     0.00       2.0-2.5     2.07       SUM     4.95	1.03 0.73 2.94 0.42 0.52 1.89	0.76 0.93 8.36 2.23 3.00	0.59 0.96 4.44	\	0.99 0.96	0.76				
2.0-2.5 0.96 SUM 4.61  120 deg  0.1-0.5 0.53 0.5-1.0 1.40 1.0-1.5 1.73 SUM 3.66  90 deg  0.1-0.5 0.91 0.5-1.0 0.65 1.0-1.5 1.31 1.5-2.0 0.00 2.0-2.5 2.07 SUM 4.95	0.73 2.94 0.42 0.52 1.89	0.93 8.36 2.23 3.00	0.96 4.44	\	0.96			0.00	0.57	0.22
SUM 4.61  120 deg  0.1-0.5 0.53 0.5-1.0 1.40 1.0-1.5 1.73 SUM 3.66  90 deg  0.1-0.5 0.91 0.5-1.0 0.65 1.0-1.5 1.31 1.5-2.0 0.00 2.0-2.5 2.07 SUM 4.95	0.42 0.52 1.89	2.23 3.00	4.44			0.00	0.80	0.21	0.89	3.00
0.1-0.5 0.53 0.5-1.0 1.40 1.0-1.5 1.73 SUM 3.66 90 deg 0.1-0.5 0.91 0.5-1.0 0.65 1.0-1.5 1.31 1.5-2.0 0.00 2.0-2.5 2.07 SUM 4.95	0.52 1.89	3.00	0.21		7.07	3.48	5.44	3.11	6.13	6.22
0.5-1.0 1.40 1.0-1.5 1.73 SUM 3.66 90 deg 0.1-0.5 0.91 0.5-1.0 0.65 1.0-1.5 1.31 1.5-2.0 0.00 2.0-2.5 2.07 SUM 4.95	0.52 1.89	3.00	0.21							
0.5-1.0 1.40 1.0-1.5 1.73 SUM 3.66 90 deg 0.1-0.5 0.91 0.5-1.0 0.65 1.0-1.5 1.31 1.5-2.0 0.00 2.0-2.5 2.07 SUM 4.95	0.52 1.89	3.00	0.31	1.13	1.01	0.34	0.31	0.21	0.43	0.97
1.0-1.5 1.73 SUM 3.66 90 deg 0.1-0.5 0.91 0.5-1.0 0.65 1.0-1.5 1.31 1.5-2.0 0.00 2.0-2.5 2.07 SUM 4.95	1.89		1.39	1.44	1.33	1.40	1.39	1.25	1.47	1.66
SUM 3.66 90 deg 0.1-0.5 0.91 0.5-1.0 0.65 1.0-1.5 1.31 1.5-2.0 0.00 2.0-2.5 2.07 SUM 4.95		1.89	1.27	1.48	1.00	2.49	1.07	0.90	1.09	1.40
90 deg 0.1–0.5 0.91 0.5–1.0 0.65 1.0–1.5 1.31 1.5–2.0 0.00 2.0–2.5 2.07 SUM 4.95	2.84	7.12	2.97	4.05	3.34	4.23	2.77	2.36	2.99	4.02
0.1–0.5 0.91 0.5–1.0 0.65 1.0–1.5 1.31 1.5–2.0 0.00 2.0–2.5 2.07 SUM 4.95										
0.5–1.0 0.65 1.0–1.5 1.31 1.5–2.0 0.00 2.0–2.5 2.07 SUM 4.95	0.85	1.36	1.82	0.97	1.00	2.51	1.73	0.10	1.16	0.91
1.0–1.5 1.31 1.5–2.0 0.00 2.0–2.5 2.07 SUM 4.95	0.87	1.52	1.40	1.11	1.00	0.46	2.93	0.27	0.51	0.94
1.5–2.0 0.00 2.0–2.5 2.07 SUM 4.95	0.63	2.04	1.36	2.19	1.24	1.33	1.40	1.78	2.00	1.31
2.0–2.5 2.07 SUM 4.95	0.70	0.97	0.96	\	0.96	0.44	0.43	0.29	0.33	3.00
SUM 4.95	0.75	2.00	2.00	2.29	1.00	2.33	1.22	1.59	1.46	1.45
60 deg	3.80	7.89	7.54	\	5.20	7.08	7.72	4.02	5.46	7.62
0.1-0.5 0.68	0.67	1.53	0.63	0.79	0.71	0.44	1.33	0.23	3.00	0.49
0.5–1.0 1.21	0.76	1.50	0.81	2.83	1.08	1.73	0.48	0.65	0.75	1.77
1.0–1.5 0.94	0.78	2.51	0.93	1.80	0.87	0.93	1.95	2.16	0.84	1.64
1.5–2.0 0.49	0.89	0.90	0.94	\	0.94	0.94	0.79	0.00	0.84	3.00
SUM 3.32	3.09	6.44	3.30	\	3.60	4.04	4.55	3.04	5.43	6.90
30 deg				,						
0.1-0.5 0.92	2.85	1.82	1.64	1.71	1.00	0.59	0.73	1.03	0.26	0.90
0.5–1.0 1.01	0.49	2.88	1.01	1.23	0.96	0.99	1.38	1.15	1.29	2.12
1.0–1.5	0.77	1.38	1.15	2.43	1.13	1.15	0.94	0.97	0.64	1.27
1.5–2.0 0.88	0.00	0.97	0.96	\	0.96	0.20	0.52	0.57	0.85	3.00
SUM 3.99	4.11	7.05	4.76	5.37	4.05	2.92	3.57	3.72	3.04	7.29
0 deg										
0.1-0.5 1.06	1.12	2.70	0.99	0.93	0.86	0.93	1.90	0.53	1.29	0.57
0.5–1.0 0.37		2.00	0.34	1.02	0.33	0.39	2.29	0.28	0.43	1.09
1.0–1.5 1.18	() 19	2.09	1.16	1.72	1.24	1.30	1.51	0.28	1.98	1.82
1.5–2.0 1.03	0.19 0.63	2.07	1.02	2.13	0.99	1.02	1.78	1.16	1.09	1.40
SUM 3.63	0.19 0.63 0.84	2.96	3.51	5.80	3.43	3.64	7.47	2.76	4.79	4.89

**Table A.4** Parameters of fitted beta distribution for  $C_{\Delta W}$ .

Lower limit	Upper limit	α	β	Location	Scale
180 deg					
0.1	0.3	0.766373	0.712087	0.54773	5.46227
0.3	0.5	0.322619	0.355631	0.644034	2.345966
0.5	0.7	0.975291	0.789488	0.899157	2.860843
0.7	0.9	0.873721	2.382317	1.49	9.146873
0.9	1.1	1.609341	1.949055	1.377633	11.74228
1.1	1.3	1.339309	0.974923	1.543853	10.57615
1.3	1.5	3.075944	4.30241	-1.09736	17.03455
1.5	1.7	0.718107	0.860154	0.66	6.598264
1.7	1.9	0.763261	0.589976	0.531321	2.068679
1.9	2.1	0.864313	0.635291	0.104816	1.295184
2.1	2.3	0.354073	0.486084	0.13	0.446408
2.3	2.5	0.997028	0.683563	0.099302	0.620698
150 deg					
0	0.5	0.245664	0.457139	0.120565	10.45944
0.5	1	0.81953	0.78929	1.821511	7.738489
1	1.5	0.836677	0.824799	0.710204	9.409796
1.5	2	0.004681	0.006184	0.680418	10.53958
2	2.5	1.330202	0.699996	1.580394	0.159606
120 deg					
0	0.5	0.58433	0.69052	5.39E-05	8.689946
0.5	1	1.182031	0.825862	0.63368	7.25632
1	1.5	0.103333	0.34008	0.047145	3.762855
90 deg					
0	0.5	0.236295	0.407887	0.401379	6.328621
0.5	1	0.275225	0.471434	-0.36955	11.67955
1	1.5	0.906038	0.830962	-0.00836	5.52836
1.5	2	1.369109	0.634243	-1.04848	3.968484
2	2.5	0.267498	0.387741	0.000662	0.969338
60 deg					
0	0.5	0.412933	1.902051	-0.89	9.432939
0.5	1	1.106368	0.675179	0.565093	2.144907
1	1.5	0.466609	0.469218	-0.448	1.738002
1.5	2	1.305435	0.99326	-0.26675	0.096752
30 deg					
0	0.5	0.054352	0.310669	-1.79	9.321019
0.5	1	0.805595	0.354453	0.150709	1.989291
1	1.5	1.145745	0.832054	-0.56349	2.04349
1.5	2	2.504823	0.161272	-0.14566	1.665659
0 deg					
0	0.5	0.587953	0.384373	-2.28229	2.932292
0.5	1	23 864 180	7.256632	-8643504	8643507
1	1.5	2344747	3.649192	-706371	706 371.9
1.5	2	0.534552	0.296358	-0.90125	1.481249

#### References

- Bayraktar, M., Yuksel, O., 2023. A scenario-based assessment of the energy efficiency existing ship index (EEXI) and carbon intensity indicator (CII) regulations. Ocean Eng. 278, 114295.
- Bayramoğlu, K., 2024. The effects of alternative fuels, cruising duration and variable generators combination on exhaust emissions, energy efficiency existing ship index (EEXI) and carbon intensity rating (CII). Ocean Eng. 302, 117723.
- Borén, C., Castells-Sanabra, M., Grifoll, M., 2022. Ship emissions reduction using weather ship routing optimisation. Proc. Inst. Mech. Eng. Part M: J. Eng. Marit. Environ. 236 (4), 856–867.
- Cheng, M., Yang, D.Y., Frangopol, D.M., 2020. Investigation of effects of time preference and risk perception on life-cycle management of civil infrastructure. ASCE-ASME J. Risk Uncertain. Eng. Syst. Part A: Civ. Eng. 6 (1), 04020001.
- Chua, Y.J., Soudagar, I., Ng, S.H., Meng, Q., 2023. Impact analysis of environmental policies on shipping fleet planning under demand uncertainty. Transp. Res. Part D: Transp. Environ. 120, 103744.
- Clarksons, 2024. Vessel speed trends. https://www.clarksons.com/media/k0ieqaia/final-year-end-presentation-2023-for-website-only.pdf. (Accessed 20 February 2025)
- Elkafas, A.G., Rivarolo, M., Massardo, A.F., 2023. Environmental economic analysis of speed reduction measure onboard container ships. Environ. Sci. Pollut. Res. 30 (21), 59645–59659.

- Esri, 2023. Esri hydrographic office: Arcgis maritime and bathymetry featured maps and apps. https://esriho.maps.arcgis.com/home/index.html. (Accessed 15 November 2023).
- Goldsworthy, B., Goldsworthy, L., 2019. Assigning machinery power values for estimating ship exhaust emissions: Comparison of auxiliary power schemes. Sci. Total Environ 657, 963–977.
- Gu, B., Liu, J., Chen, J., 2023. Scenario-based strategies evaluation for the maritime supply chain resilience. Transp. Res. Part D: Transp. Environ. 124, 103948.
- Guo, Z., Hong, M., Zhang, Y., Shi, J., Qian, L., Li, H., 2024. Research on safety evaluation and weather routing optimization of ship based on roll dynamics and improved A\* algorithm. Int. J. Nav. Archit. Ocean. Eng. 100605.
- Ha, J., Roh, M.-I., Lee, H.-W., 2024. Ship route planning for collision avoidance based on the improved isochrone method. Int. J. Nav. Archit. Ocean. Eng. 16, 100613.
- Han, S.W., Kwak, D.H., Byeon, G.-w., Woo, J.H., 2024. Forecasting shipbuilding demand using shipping market modeling: A case study of LNGC. Int. J. Nav. Archit. Ocean. Eng. 16, 100616.
- Hua, R., Yin, J., Wang, S., Han, Y., Wang, X., 2024. Speed optimization for maximizing the ship's economic benefits considering the carbon intensity indicator (CII). Ocean Eng. 293, 116712.
- Irena, K., Ernst, W., Alexandros, C.G., 2021. The cost-effectiveness of CO2 mitigation measures for the decarbonisation of shipping. The case study of a globally operating ship-management company. J. Clean. Prod. 316, 128094.
- Islam, H., Rahaman, M.M., Akimoto, H., Islam, M.R., 2017. Calm water resistance prediction of a container ship using reynolds averaged navier-stokes based solver. Procedia Eng. 194, 25–30.
- ISO, 2015. ISO 15016:2015 ships and marine technology Guidelines for the assessment of speed and power performance by analysis of speed trial data.
- Jeong, D.-G., Roh, M.-I., Yeo, I.-C., Kim, K.-S., Lee, J.-S., 2025. A route planning method for small ships in coastal areas based on quadtree. Int. J. Nav. Archit. Ocean. Eng. 100647.
- Jon, M.H., Yu, C.I., 2023. Optimization of ship energy efficiency considering navigational environment and safety. In: Proceedings of the 5th International Conference on Numerical Modelling in Engineering: Volume 2: Numerical Modelling in Mechanical and Materials Engineering, NME 2022, 23–24 August, Ghent University, Belgium. Springer, pp. 1–15.
- Kristensen, H.O., 2017. Energy Demand and Exhaust Gas Emissions of Marine Engines. Technical Report, Technical University of Denmark.
- Kurosawa, K., Uchiyama, Y., Kosako, T., 2020. Development of a numerical marine weather routing system for coastal and marginal seas using regional oceanic and atmospheric simulations. Ocean Eng. 195, 106706.
- Lashgari, M., Akbari, A.A., Nasersarraf, S., 2021. A new model for simultaneously optimizing ship route, sailing speed, and fuel consumption in a shipping problem under different price scenarios. Appl. Ocean Res. 113, 102725.
- Li, X., Sun, B., Guo, C., Du, W., Li, Y., 2020. Speed optimization of a container ship on a given route considering voluntary speed loss and emissions. Appl. Ocean Res. 94, 101995
- Li, X., Zhao, Y., Cariou, P., Sun, Z., 2024. The impact of port congestion on shipping emissions in Chinese ports. Transp. Res. Part D: Transp. Environ. 128, 104091.
- Liu, S., Papanikolaou, A., 2020. Regression analysis of experimental data for added resistance in waves of arbitrary heading and development of a semi-empirical formula. Ocean Eng. (ISSN: 0029-8018) 206, 107357.
- Mannarini, G., Carelli, L., Orović, J., Martinkus, C.P., Coppini, G., 2021. Towards least-CO2 ferry routes in the Adriatic sea. J. Mar. Sci. Eng. 9 (2), 115.
- MEPC, 2021. Resolution mepc.328(76) amendments to the annex of the protocol of 1997 to amend the international convention for the prevention of pollution from ships,1973, as modified by the protocol of 1978 relating thereto.
- MEPC, 2022a. Resolution mepc.338(76) 2021 guidelines on the operational carbon intensity reduction factors relative to reference lines (CII reduction factors guidelines, G3).
- MEPC, 2022b. Resolution mepc.352(78) 2022 guidelines on operational carbon intensity indicators and the calculation methods (CII guidelines, G1).
- MEPC, 2022c. Resolution mepc.353(78) 2022 guidelines on the reference lines for use with operational carbon intensity indicators (CII reference lines guidelines, G2).
- MEPC, 2022d. Resolution mepc.354(78) 2022 guidelines on the operational carbon intensity rating of ships (CII rating guidelines, G4).
- MEPC, 2023. Resolution mepc.377(80) 2023 IMO strategy on reduction of GHG emissions from ships.
- Mittendorf, M., Nielsen, U.D., Bingham, H.B., Liu, S., 2022. Towards the uncertainty quantification of semi-empirical formulas applied to the added resistance of ships in waves of arbitrary heading. Ocean Eng. 251, 111040.
- Moradi, M.H., Brutsche, M., Wenig, M., Wagner, U., Koch, T., 2022. Marine route optimization using reinforcement learning approach to reduce fuel consumption and consequently minimize CO2 emissions. Ocean Eng. 259, 111882.
- OOCL, 2023. Orient overseas container line limited: Service routes. https://www.oocl.com/eng/ourservices/serviceroutes/tptday4/Pages/default.aspx. (Accessed 1 November 2023)
- Pan, J.-J., Zhang, Y.-F., Fan, B., 2022. Strengthening container shipping network connectivity during COVID-19: A graph theory approach. Ocean & Coastal Management 229, 106338.
- Sen, P., Yang, J.-B., 2012. Multiple Criteria Decision Support in Engineering Design. Springer Science & Business Media.

- Seo, J.H., Seol, D.M., Lee, J.H., Rhee, S.H., 2010. Flexible CFD meshing strategy for prediction of ship resistance and propulsion performance. Int. J. Nav. Archit. Ocean. Eng. 2 (3), 139–145.
- Sheng, Z., Liu, Y., 2004. Principles of Naval Architecture. Shanghai Jiao Tong University Press.
- Sheng, D., Meng, Q., Li, Z.-C., 2019. Optimal vessel speed and fleet size for industrial shipping services under the emission control area regulation. Transp. Res. Part C: Emerg. Technol. 105, 37–53.
- SIMMAN, 2008. MOERI container ship (KCS). http://www.simman2008.dk/KCS/container.html. (Accessed 13 September 2023).
- Sun, W., Tang, S., Liu, X., Zhou, S., Wei, J., 2022. An improved ship weather routing framework for CII reduction accounting for wind-assisted rotors. J. Mar. Sci. Eng. 10 (12), 1979.
- Sun, L., Wang, X., Lu, Y., Hu, Z., 2023. Assessment of ship speed, operational carbon intensity indicator penalty and charterer profit of time charter ships. Heliyon 9 (10).
- Tang, H., Hu, J., Li, X., 2024. A novel method for generating inland waterway vessel routes using AIS data. Int. J. Nav. Archit. Ocean. Eng. 16, 100621.
- Tran, T.T., Browne, T., Veitch, B., Musharraf, M., Peters, D., 2023. Route optimization for vessels in ice: Investigating operational implications of the carbon intensity indicator regulation. Mar. Policy 158, 105858.
- Tsai, Y.-M., Lin, C.-Y., 2023. Effects of the carbon intensity index rating system on the development of the northeast passage. J. Mar. Sci. Eng. 11 (7), 1341.

- Wan, Z., Su, Y., Li, Z., Zhang, X., Zhang, Q., Chen, J., 2023. Analysis of the impact of Suez Canal blockage on the global shipping network. Ocean & Coastal Management 245, 106868.
- Wang, B., Liu, Y., Dai, W., Li, J., 2025. Incremental route planning based on daily risk assessment for Arctic navigation. Ocean Eng. 320, 120294.
- Wang, H., Mao, W., Eriksson, L., 2019. A three-dimensional Dijkstra's algorithm for multi-objective ship voyage optimization. Ocean Eng. 186, 106131.
- Wei, Q., Liu, Y., Dong, Y., Li, T., Li, W., 2023. A digital twin framework for real-time ship routing considering decarbonization regulatory compliance. Ocean Eng. 278, 114407
- Wetterdienst, D., 2023. Open data area of the climate data center. https://www.dwd.de/EN/ourservices/cdc/cdc.html. (Accessed 1 November 2023).
- You, Y., Lee, J.C., 2022. Activity-based evaluation of ship pollutant emissions considering ship maneuver according to transportation plan. Int. J. Nav. Archit. Ocean. Eng. 14, 100427.
- Yuan, Q., Wang, S., Peng, J., 2023. Operational efficiency optimization method for ship fleet to comply with the carbon intensity indicator (CII) regulation. Ocean Eng. 286, 115487.
- Zheng, C.-w., Li, X.-h., Azorin-Molina, C., Li, C.-y., Wang, Q., Xiao, Z.-n., Yang, S.-b., Chen, X., Zhan, C., 2022. Global trends in oceanic wind speed, wind-sea, swell, and mixed wave heights. Appl. Energy 321, 119327.
- Zhu, Y., Wu, P., 2021. Design on construction scheme of 3600 TEU container ship (in Chinese). Shipbuild. Technol. Res. 54 (1), 21–27.